Review Article Open Access

V.A. Barachevsky\*

# Nanophotochromism

**Abstract:** The review presents the state-of-the-art analysis of investigations in the field of a new line of research of photochromism – nanophotochromism. The design, properties, and possible applications of photochromic nanoparticles prepared by different methods with the use of photochromic substances (aggregates, host-guest, and polymer systems, solid nanoparticles) as well as core-shell photochromic nanostructures based on polymers, silica, quantum dots, doped upconversion nanocrystals, and Ag, Au, etc. nanoparticles have been reviewed.

**Keywords:** photochromism; photochromic nanoparticles; core-shell photochromic nanoparticles design; photoswitching; aggregates; polymer systems, host-guest systems

DOI 10.1515/oph-2015-0003
Received November 4, 2014; accepted December 19, 2014

# 1 Introduction

Photochromism is a very important phenomenon for different applications in photonics. The applications are based on reversible phototransformations of photochromic compounds between two states and changes of their properties that accompany these transformations

At present, systems and materials containing photochromic nanopatricles have become highly significant. Among these are nanodimensional particles of photochromic substances, including aggregates, and coreshell systems. As a core, inorganic nanoparticles of gold, silver, metal oxides, quantum dots (QD), and also polymeric nanoparticles are used. The shell consists of photochromic molecules or their aggregates connected to a core surface either chemically or physically. Photochromic nanoparticles with photocontrolled fluorescence arouse a special interest because the fluorescence technique is becoming a leading strategy in biological diagnosis, imaging, and detection applications.

This paper is a state-of-the-art review which presents results of studying photochromic nanoparticles including author's own data. The results of earlier research are also surveyed in some other reviews [1–13].

# 2 Photochromic nanoparticles: properties and applications

# 2.1 Nanoparticles based on photochromic substances

#### Aggregates

The most known photochromic nanoparticles are aggregates of photochromic organic compounds [14]. These compounds experience reversible photoinduced transformations between two states, Sch. 1A and Sch. 1B.

Scheme 1

The photoinduced colored merocyanine form B absorbing visible irradiation is formed from a colorless form A as a result of photodissociation of the –C–O– bond of the pyran heterocycle under UV radiation, and this is followed by spontaneous isomerization of the *cis*- form to the *trans* one. The colored form B can be converted back to the initial colorless form A upon absorption of visible light or spontaneously during the dark relaxation, which is accelerated by heating.

The J-aggregates of nitro-substituted indoline spiropyrans Sch. 2 with long alkyl substituents are of special interest [15].

The narrow absorption bands of J-aggregates of these photochromic compounds (Fig. 1) made it possible prepare a specimen of the multilayered optical disk providing fre-

<sup>\*</sup>Corresponding Author: V.A. Barachevsky: Photochemistry Center of the Russian Academy of Sciences, Moscow, 119421, Novatorov Str., 7a, bld.1, E-mail: barya@photonics.ru

$$R_1$$
 $N_2$ 
 $R_2$ 
 $R_3$ 
 $R_4$ 

#### Scheme 3

quency selective writing, rewriting and readout of optical information.

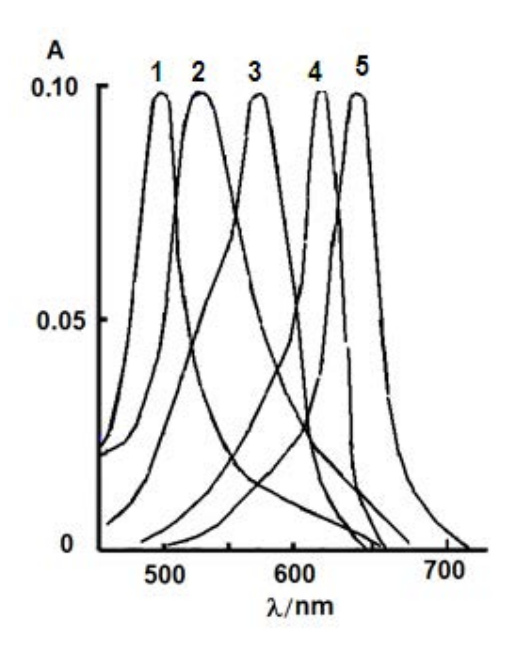


Figure 1: Absorption spectra of J-aggregates of the photoinduced merocyanine form for nitro-substituted spiropyrans containing different substituents:  $R_1 = OCH_3$ ;  $R_2 = H$ ;  $R_3 = C_{18}H_{37}$ ;  $R_4 = CH_2OCOC_{21}H_{43}(1)$ ;  $R_1 = CI$ ;  $R_2 = CI$ ;  $R_3 = CH_3$ ;  $R_4 = CH_2OCOC_{21}H_{43}(2)$ ;  $R_1 = H$ ;  $R_2 = H$ ;  $R_3 = (CH_2)_3SO_3$ ;  $R_4 = H(3)$ ;  $R_1 = H$ ;  $R_2 = H$ ;  $R_3 = C_{18}H_{37}$ ;  $R_4 = CH_2OCOC_{21}H_{43}(4)$ ;  $R_1 = Br$ ;  $R_2 = Br$ ;  $R_3 = C_{18}H_{37}$ ;  $R_4 = CH_2OCOC_{21}H_{43}(5)$ 

The photoinduced aggregation of the photochromic spiro compounds Sch. 2 was used to fabricate photocontrolled photon crystals [16]. The photon crystals were created using spherical  $SiO_2$  nanoparticles with a diameter of 195 – 275 nm coated with molecules of photochromic spiropyrans forming J-aggregates of the merocyanine form at 350°C. A coating up to 10 microns thick was deposited by vacuum evaporation technique.

The photoinduced change of the refractive index of a photochromic compound incorporated into the structure of a photon crystal is the cornerstone of this application. There is a change in the absorption spectrum of merocyanine form B and the corresponding change in the dispersive curve depending on the extent of photoinduced aggregation (Fig. 2). As a result of J-aggregation, the photoinduced absorption spectrum is reversibly displaced from 725 to 762 nm.

The J-aggregation of molecules of the coumarin derivatives of spiropyran Sch. 3 showing resonance fluorescence in polymolecular layers (Fig. 3) provides generation of the second harmonic of neodymium laser radiation [17].

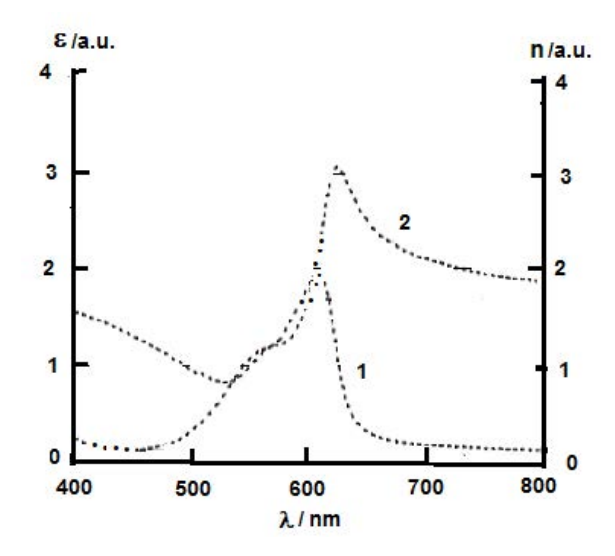


Figure 2: Absorption spectrum (1) and dispersion curve of the refractive index (2) for the photoinduced merocyanine form of nitro-substituted spiropyran Sch. 2 ( $R_1$  =H;  $R_2$  =H;  $R_3$  = $C_{18}H_{37}$ ;  $R_4$  = $CH_2OCOC_{21}H_{43}$ ).

The aggregation of molecules of the azobenzene–phthalocyanine dyads was used for realization of effective third order nonlinearity [18].

All results suggest that photochromic compounds have a potential in the field of nonlinear optics applications.

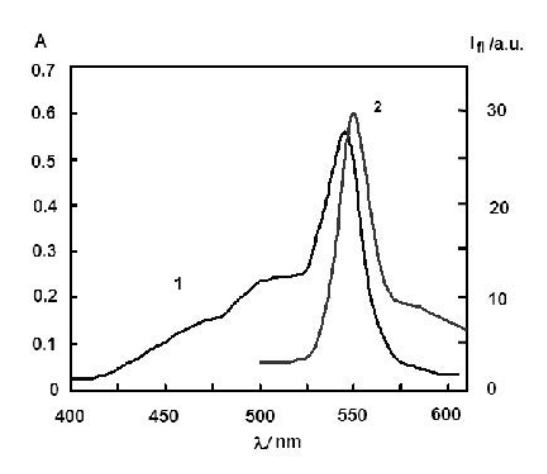


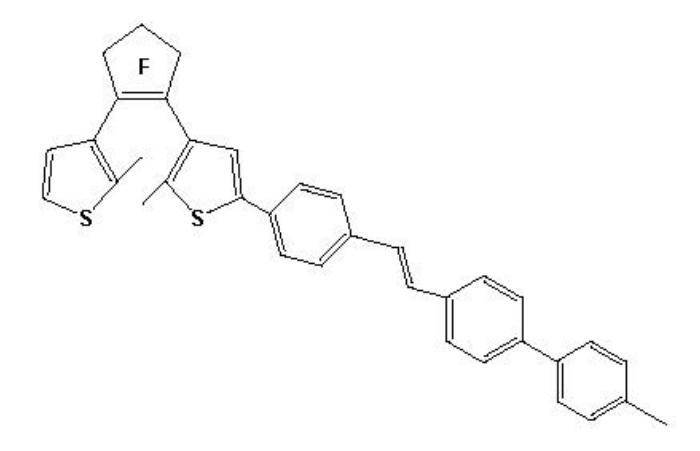
Figure 3: Absorption (1) and fluorescence (2) spectra of J-aggregates of the merocyanine form of spiropyran Sch. 3 in a polymolecular layer.

The aggregation of cyano-containing diarylethene derivative Sch. 4 in organic nanoparticles prepared by a reprecipitation method results in enhanced fluorescence and bistable photoswitching [19]. Unlike this compound, the conventional analog without the cyano-group [5] shows significant concentration fluorescence quenching in the nanoparticles. It is connected with the formation of J- and H-aggregates, respectively.

Upon the photochromic ring closure of compound Sch. 4, fluorescence intensities of J-aggregates in tetrahydrofuran or polymethyl methacrylate (PMMA) (Fig. 4) were greatly and reversibly reduced.

Scheme 4

Aggregation-induced emission and repeated fluorescence switching are exhibited by a dithienylethene—tetraphenylethene conjugate Sch. 6 [20]. In contrast to the lack of fluorescence in solution, in the solid state, this con-



#### Scheme 5

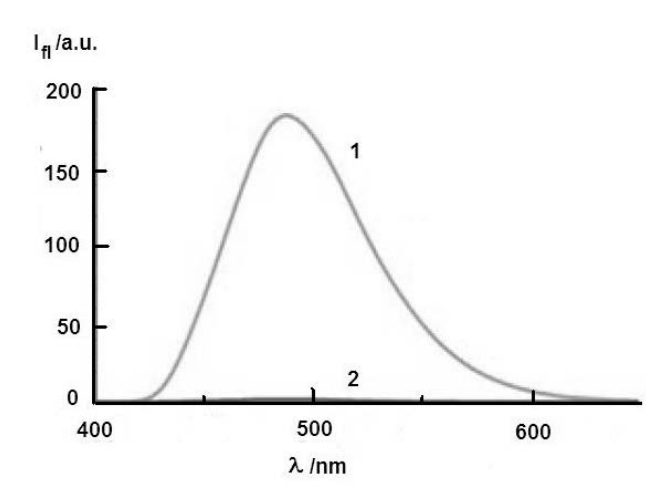


Figure 4: Fluorescence spectra of compound Sch. 4 in the PMMA film before (1) and after UV irradiation (2).

#### Scheme 6

jugate exhibits a strong emission at 520 – 540 nm which appeared after UV irradiation and excitation by 440 nm light and restored under visible irradiation. Reversible fluorescence modulation was observed according to photochromic transformations.

#### **Host-guest systems**

The aggregation of spiropyran molecules was observed for axial complexes between photochromic molecules with a long-chain alkyl substituents Sch. 7 and  $\alpha$ -,  $\beta$ -, and  $\gamma$ -cyclodextrins [21, 22]. The H-aggregates appeared at relatively low concentrations of photochromic spiropyrans. The J-aggregates are formed at high concentrations and are characterized by absorption bands of the photoinduced merocyanine form at 700, 650, and 630 nm for  $\alpha$ -,  $\beta$ -, and  $\gamma$ - cyclodextrins, respectively.

$$R = -CH_3$$
; -n  $-C_{16}H_{33}$ ; - $(CH_2)_4$  -NEt<sub>3</sub>

#### Scheme 7

$$\sim$$

X= -NO2, -CN, -CHO

#### Scheme 8

The inclusion of halogen-substituted spiropyrans as guests in  $\gamma$ -cyclodextrin allows photochromism to occur in the solid state [23]. The solid host cage dramatically increased the thermal lifetime and hindered the photodegradation as compared with solutions of these photochromic compounds. The data obtained indicate that hydrogen bonding is present between  $\gamma$ -cyclodextrin and photochromic spiropyran. The observed thermal stabilization depends on the nature of substituents in spyropyrans Sch. 8 [24].

The photochromic inclusion complexes were detected in a study of the reaction between 1,3-dihydro-1,3,3-trimethylspiro[2H]-indole-2,3'-[3H]-naphtho[2,1-b][1,4]oxazine Sch. 9 and  $\gamma$ - cyclodextrin [25].

#### Scheme 9

The film based on this complex showed normal photochromism but spontaneous bleaching of the photoin-duced merocyanine form in the  $\gamma$ -cyclodextrin cavity was nearly an order order of magnitude faster than outside the cavity.

The introduction of 2,2'-dimethyl-3,3'-(perfluoropentene-1,2-diyl)bis(benzo[b]thiophene-6-sulfonate Sch. 10 into  $\beta$ - and  $\gamma$ -cyclodextrins leads to the enhancement of the quantum yield of the photoinduced closed form [26, 27]. This is related to favorable antiparallel conformation of diarylethene in the cavity.

Scheme 10

Scheme 11

 $\gamma$ –Cyclodextrin containing photochromic 1,2-bis(1-benzothiophen-3-yl) perfluorocyclopentene, prepared using compound Sch. 11, exhibited reversible photoinduced circular dichroism and optical rotation [28].

An increase in the quantum yield for the cyclization reaction and photoinduced change from negative to positive circular dichroism were found for dithienylethene-bis(trimethyl-ammonium) iodide in the  $\beta$ -cyclodextrin cavity [29, 30].

The  $\beta$ -cyclodextrin dimer tethered by photochromic diarylethene was synthesized as a potential tunable receptor [31]. This dimer was found to exhibit pronounced photochromic properties.

#### Solid nanoparticles

The vacuum evaporation of thermally irreversible photochromic fulgide has been used to prepare large-size nanostructured photochromic materials [32]. The photochromic layer was deposited on the surface of a 2-22 nm-thick organic film preliminary punched by the photolithography method. The recording medium for the optical disks providing a recording density of optical information of 74 GB per square inch was manufactured in this way.

Photochromic nanoparticles may be prepared by selective doping of photochromic compounds, in particular, *cis-*1,2-dicyano-1,2-bis(2,4,5-trimethyl-3-thienyl)ethane Sch. 12, into nanostructures of diblock copolymer films based on poly(phenyl metacrylate), poly(methyl methacrylate), poly(*tert*-butyl methacrylate), polystyrene, poly(4-methylstyrene), poly(*p*-tert-butylstyrene), and polycarbonate by vacuum vaporization of a photochromic compound [25, 33].

Scheme 12

Nanoparticles of diarylethene Sch. 12 and two salicylidene anilines Sch. 13 were prepared by vapor deposition [34]. The nanocrystals (100 – 500 nm) of salicylideneanilines showed photochromic transformations similar to those of bulk crystals. A thin layer (65 nm) of *cis*-1,2-

Scheme 13

dicyano-1,2-bis(2,4,5-trimethyl-3-thienyl)ethane with and without Au nanoparticles exhibited spectral transformations in the visible range.

Nanoparticles containing spiropyrans bearing hydrophobic alkyl chains Sch. 14 were prepared by direct precipitation [35]. According to this method, an acetonitrile solution of spiropyran was precipitated into water to give nanoparticles of the 198 nm size. To improve the stability and drug loading efficiency, hybrid spiropyran/lipid-polyethylene glycol nanoparticles were prepared using the ultrasonication method. It was found that these nanoparticles undergo a reversible volume change from 150 to 40 nm upon UV irradiation because of spiropyran photochromic transformations. This feature was used for photoinduced drug release inside cells.

Scheme 14

The molecules of thermally irreversible photochromic 1,3-bis(3-thienyl) perfluorocyclopentene derivatives dissolved in tetrahydrofuran form H-aggregates of 60 – 230 nm size depending on temperature (283 – 298) during their reprecipitation in water [36]. The formation of H-aggregates is supported by the blue spectral shift of the absorption maximum of the closed form and decreasing fluorescence efficiency of the open form of diarylethene.

The reprecipitation method was used to prepare photochromic nanoparticles representing polyamorphous structures of 1,2-bis(2-methyl-5-methoxyphenyl-3-thienyl) perfluorocyclopentene [37].

Spiropyran nanocrystals based on (1,3-dihydro-1,3,3,5',6'-pentamethylspiro[2H-indole-2,2'-[2H-b]pyrano[3,2-b]pyridinium]indole) Sch. 15 embedded in sol-gel matrices provided high photoconversion efficiency and increasing lifetime of the merocyanine form up to 41 h as compared with microcrystals (6 h) because of the crystalline structure of nanocrystals [38].

$$\begin{array}{c|c} & & & \\ & & & \\ & & & \\ & & & \\ & & \\ & & \\ & & \\ & & \\ & & \\ & & \\ & & \\ & & \\ & & \\ & & \\ & & \\ & & \\ & & \\ & & \\ &$$

#### Scheme 15

The laser ablation method used to was nanoparticles from photochromic prepare substances under irradiation at 355 and 532 nm. In particular, nanoparticles of 1,2-bis-(5'-ethoxy-2'-(2'pyridyl)thiaazolylperfluorocyclopentene were tained by this method in an aqueous solution containing dodecyltrimethylammonium bromide [39]. This compound photoswitched reversibly in the bulk crystal and in a colloidal solution of nanoparticles. The method of Laser ablation under radiation at 355 nm was used to prepare nanoparticles of 1,2-bis[4'-methyl-2'-(2"pyridyl)thiazolylperfluoroceclopentene with 25 nm diameter from a suspension of a microcrystalline powder in a water-sodium dodecylsulfate medium [40]. The colloidal aqueous suspension is characterized by quantum yields of photochromic transformations  $\varphi_{AB}$  =0,20 and  $\varphi_{BA}$  =0,96. The fluorescence quantum yield was  $\varphi^{fl}$  =0,017. This compound is not photochromic as the bulk solid and manifests only weakly fluorescence in acetonitrile ( $\varphi^{fl}$  =0,005).

Nanorods of photochromic N-(3,5-di-*tert*-butylsalicylidine)-4-aminopyridine **15** prepared by laser ablation exhibit intermediate photochromic properties as compared with solution and the solid and fatigue-resistant photoswitching [41].

Scheme 16

It was shown that photochromic nanorods can be fabricated either by laser irradiation for a short period of time or simply by continuous irradiation at a suitable wavelength [42]. These nanoparticles are characterized by strong fatigue-resistant switching of photochromic properties.

The photoresponsive spiropyran-containing nanoparticles of 30 – 60 nm size were successfully synthesized by a facile one-step miniemulsion polymerization [43]. It was shown that the nanoparticle dispersion exhibits photoinduced enhanced reversible transformations, high photostability, and relatively fast photo-responsive properties as compared with the same species in aqueous solution.

#### Polymer systems

Nanoparticles based on ethyl-cellulose-1,3-dihydro-1,3,3,4,5 (and 1,3,3,5,6)-pentamethyl-spiro-[2H-indole-2,3'-(3H)naphtha(2,1-b)(1,4)oxazine Sch. 17 as well as photostabilizer Tinuvin 144 were prepared [44] by using an oil-in-water emulsion and following solvent evaporation [45]. These nanoparticles were used for application in a screen-printing paste for textile dying.

$$\begin{array}{c|c} & & & \\ & & & \\ N - cH_2 - cH_2 - c \\ 0 & & & \\ \end{array} - \begin{array}{c} c - c - c - c \\ 0 & & \\ \end{array} - \begin{array}{c} C - c - c \\ 0 & & \\ \end{array}$$

Scheme 17

It was shown that photochromic nanoparticles based on poly(methyl methacrylate) and ethylcellulose containing photochromic 1,3-dihydro-1,3,3,4,5-pentamethyl-spiro-[2H-indole-2,3'-[3H]naphtha[2,1-b][1,4]oxazine and bifunctional hindered amine light stabilizer Tinuvin 144 are characterized by increase in the lifetime of the photoinduced merocyanine form (by a factor of 10 as compared with organic solutions) and considerable enhancement of fatigue resistance [46].

Photochromic polymer nanoparticles based on novel naphthopyran Sch. 18 were prepared by miniemulsion copolymerization with methyl methacrylate and n-butyl methacrylate [47].

Using 5-(1,3-dihydro-3,3-dimethyl-6-nitrospiro[2y-1benzopyran-2,2'-(2H)-indole])ethyl acrylate polymer

Scheme 18

nanoparticles of diameter 40-400 nm have been prepared by emulsion polymerization [48]. These nanoparticles undergo reversible fluorescence photoswitching of the merocyanine form ( $\varphi^{fl}=0,24$ ) according to photochromic transformations of spiropyran.

H-aggregation is the basis of self-assembled nanotubes prepared with the use of a photochromic bisthienylene-functionalized perylene diimide dyad Sch. 19 [49]. The observed green emission of the of diarylethene units at 520 nm could be controlled by UV and visible light.

Scheme 19

Photochromic electrospun poly(methyl methacrylate) nanofibers of 90 nm size exhibiting reversible fluorescence modulation according to photochromic transformations were prepared with the use of 1',3'-dihydro-1',3',3'-trimethyl-6-nitrospiro[2H-1-benzopyran-2.2'-(2H)-indole] [50]. These nanofibers open up new possibilities for implementation of photocontrolled nanometer-scale elements for integrated nanooptics. Photochromic 1,2-bis(2-methyl-5-(4-methoxyphenyl)-3-thienyl)perfluorocyclopentene doped into polymer nanofibers was used for evaluation of the orientation of molecules in the electrospun nanofibers [51].

A new type of photoswitchable nanoprobes based on binary composite nanococktails were developed for in vivo applications [52]. These binary nanococktails contain cyanovinylene-backboned polymers Sch. 20 as a concentrated fluorescence emitter and 1,2-bis-(2.4-dimethyl-5-phenyl-3-thienyl)-3.3.4.4.5.5-hexafluoro-1cyclopentene Sch. 21 as a photoswitching modulator. The aggregated polymer nanoparticles manifest bright solidstate fluorescence depending on the aromatic structure of dialdehyde monomer used. The polymer prepared from the biphenylene monomer emits at 585 nm ( $\varphi^{fl}$  =0.6). The use of dioctylphenylene monomer leads to formation of a polymer emitting in the NIR spectral range ( $\lambda_{max}^{fl}$  =728 nm,  $\varphi^{fl}$  =0.2). The overlap of these fluorescence bands with the absorption band of the closed diarylethene isomer  $(\lambda_{max}$  =580 nm) provided the efficient fluorescence resonance energy transfer (FRET)-based fluorescence quenching. The developed nanococktails showed reversible highcontrast photoswitching and nondestructive fluorescent readout of a fluorescence signal.

$$\begin{array}{c|c} & & & & & & & \\ & Ar & & & & & \\ & NC & & & & \\ & & & & & \\ & & & & & \\ & & & & & \\ & & & & & \\ & & & & & \\ & & & & \\ & & & & \\ & & & & \\ & & & & \\ & & & \\ & & & \\ & & & \\ & & & \\ & & & \\ & & & \\ & & & \\ & & \\ & & & \\ & & \\ & & \\ & & \\ & & \\ & & \\ & & \\ & & \\ & & \\ & & \\ &$$

Scheme 20

Scheme 21

Based on photochromic fulgides, two types of photochromic nanostructures, namely, amorphous dots of a tunable size and nanocrystals, were prepared via UHV-deposition on helium-cooled surfaces [53]. Both forms

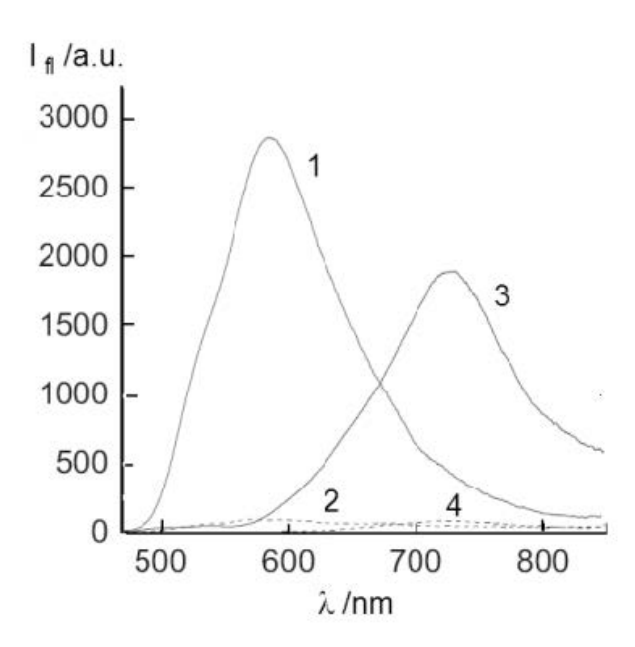


Figure 5: Fluorescence spectra for mixtures of Sch. 20a and Sch. 21 (1,2) and Sch. 20b and Sch. 21 (3,4) in nanococktails (1:3 weight %) before (1,3) and after UV irradiation (2,4)

were stable at room temperature and manifested photochromism.

# 2.2 Core-shell photochromic nanoparticles

For the preparing of amphiphilic core-shell type nanoparticles, coatings of photochromic compounds have been developed [19, 54, 55]. A number of these nanoparticles exhibit reversible fluorescence switching [19, 56–58].

## Polymeric nanoparticles

Amphiphilic core-shell nanopatricles containing spiropyran Sch. 22 moieties consist of hydrophilic and biocompatible poly(ethyleneimine) chain segments forming the shell and a hydrophobic copolymer of methyl methacrylate, spiropyran-linked methacrylate, and cross-linker forming the core [59]. Polymeric nanoparticles were prepared by one-step miniemulsion polymerization. Hydrophobic fluorescent dye based on nitrobenzoxadiazolyl groups Sch. 23 incorporated into the core was used as a fluorophore. Modulation of fluorescence intensity is achieved by the FRET effect (Fig. 6).

The diameter of the nanoparticles can be varied from 40 to 80 nm [59] - [61]. 9,10-Diphenylanthracene was also used as a fluorophore [62].

Scheme 22

Scheme 23

Spiropyran Sch. 24 ( $\lambda^{fl}$  =600 – 700 nm,  $\varphi^{fl}$  =0.18) and fluorescent perylene diimide Sch. 25 ( $\lambda^{fl}$  =535 nm,  $\varphi^{fl}$  =0.90) were incorporated to generate optically addressable dual-color fluorescent system within the hydrophobic core [55].

Core-shell polymeric nanoparticles, covalently functionalized with photochromic spiropyrans Sch. 26, Sch. 27 and spirooxazines Sch. 28, Sch. 29 in their hydrophobic cores, were fabricated by incorporating photochromic compounds into hydrophobic cavities by modified microemulsion polymerization [63]. It was shown that the fluorescence properties of polymeric photochromic nanopar-

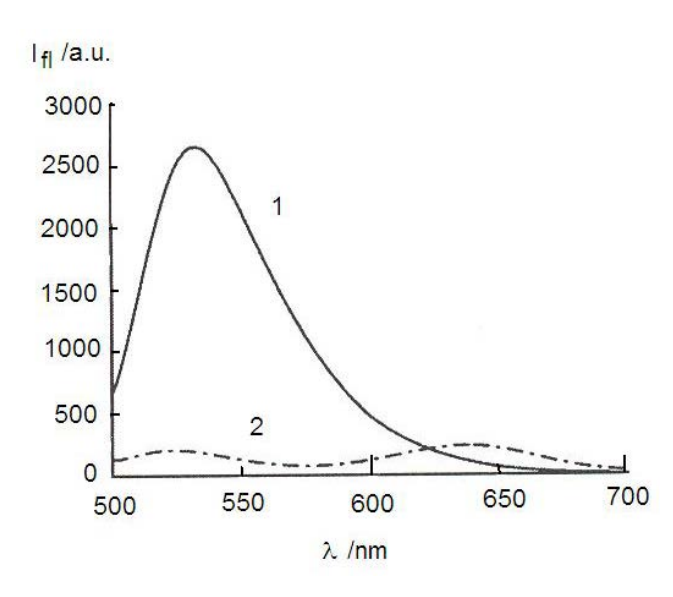


**Figure 6:** Fluorescence spectra of nanoparticles based on spiropyran Sch. 22 (C=1,2. $10^{-3}$  M) and fluorophore – hydrophobic nitrobenzoxadiazolyl dye Sch. 23 (C=1,07. $10^{-3}$  M) in aqueous dispersion under visible (1) and UV irradiation (2).

Scheme 24

Scheme 25

ticles depend on the molecular structure of photochromic compounds (Table 1).

The electron-donating and electron-withdrawing abilities of substituted groups are responsible for the tunable dual-color photoswitching performance.

Photochromic nanoparticles based on 5-(1,3-dihydro-3,3-dimethyl-6-nitrospiro[2H-1-benzopyran-2,2'-(2H)-indole)ethyl acrylate exhibiting strong photoinduced flu-

SP1: 
$$R_1 = H$$
;  $R_2 = NO_2$   
SP2:  $R_1 = OCH_3$ ;  $R_2 = NO_2$   
SP3:  $R_1 = OCH_3$ ;  $R_2 = CN$   
SP4:  $R_1 = H$ ;  $R_2 = CN$ 

#### Scheme 26

$$\begin{array}{c} R_{1} \\ N \\ O \end{array} \qquad \begin{array}{c} SP5: R_{1} = 0 \, CH \; ; \; R_{2} = NO_{2} \\ SP6: R_{1} = 0 \, CH_{3} \; ; \; R_{2} = H \\ SP7: R_{1} = H; \qquad R_{2} = NO_{2} \end{array}$$

Scheme 27

Scheme 28

orescence in hydrophobic nanocavities of polymers were used for reversible laser two-photon fluorescence excitation (780 nm) and one-photon decrease in the fluorescence intensity (488 nm) [64].

Conjugated polymers, in particular poly(*p*-phenylenevinylene), as fluorophores in combination with photochromic azo dyes, spirooxazines, and diarylethenes may be used for photocontrolled reversible fluorescence intensity modulation [65].

Nanoparticles containing photochromic *cis*-1,2-bis(2,4,5-trimethyl-3-thienyl)ethane Sch. 30 ( $\lambda_{max}^{abs}$  =518 nm) and fluorescent dye Sch. 31 ( $\lambda_{max}^{fl}$  =503 nm)

Table 1: Fluorescence maxima of photochromic spirocompounds

Compound									S02
$\lambda_A^{fl.max}$ , nm									440
$\lambda_B^{fl.max}$ , nm	665	665	665	650	615	605	605	NA	NA

Note:  $\lambda_A^{fl.max}$  and  $\lambda_B^{fl.max}$  –wavelengths of fluorescence maxima for initial close and photoinduced open forms of spirocompounds

#### Scheme 29

prepared by miniemulsion polymerization exhibit light-controlled on-off fluorescence switching even when embedded in hydrogels [58].

Scheme 30

Highly fluorescent chameleon nanoparticles were prepared from organic fluorophores Sch. 32 – Sch. 34 and diarylethene Sch. 35 using the FRET effect [66].

Photochromic diarylethene Sch. 36 was used as a "toggle switch" for biocompatible fluorescence nanoparticles based on fluorescence polymer Sch. 37 and amphiphilic polystyrene polymer Sch. 38 [67]. These photochromic nanoparticles may be used for imaging of living cells, such as neurons.

Scheme 31

Scheme 32

Scheme 33

Scheme 34

Spirobenzopyran photochromic nanoparticles containing fluorophores with noncovalent assembling Sch. 39 – Sch. 42 were embedded in the nanoscale cross-linked polymeric matrix by means of modified

n

Scheme 41

Scheme 37

miniemulsion polymerization [68]. Nanopatricles exhibit high-contrast fluorescent photoswitching.

The same results were obtained with FRET-mediated multicolor and photoswitchable fluorescent polymer nanoparticles based on photochromic spiropyran Sch. 43 containing organic fluorophores, namely 4-ethoxy-9-allyl-1,8-naphthalimide Sch. 44 and alkyl-(7-nitro-benzo[1,2,5]-oxadiazol-4-yl)-amine Sch. 45 [69]. These nanoparticles

were prepared by one-step miniemulsion polymerization

via methyl methacrylate copolymerization.

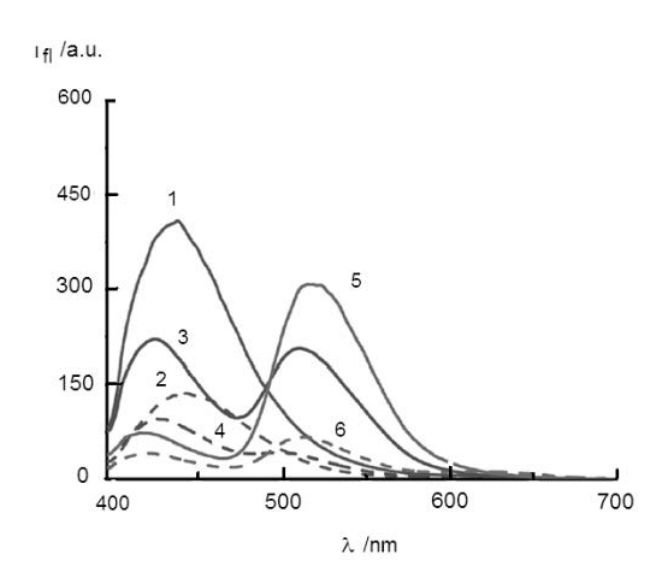
NEt<sub>2</sub>

Figure 7 illustrates the fluorescence spectra of partial FRET-mediated nanoparticles based on spiropyran Sch. 43 and different concentration ratios of fluorophores Sch. 44 and Sch. 45 under single wavelength excitation. It is seen that samples are characterized by different emission colors, which disappear under UV irradiation.

#### Scheme 43

#### Scheme 44

#### Scheme 45



**Figure 7:** Fluorescence spectra of aqueous dispersions of nanoparticles under visible (1, 3, 5) and UV irradiation (2,4,6) for samples containing spiropyran Sch. 43 (C= $5.10^{-3}$  M) together with Sch. 44 (C= $2.10^{-4}$ M) (1,2); Sch. 44 (C= $2.10^{-4}$ M) and Sch. 45 (C= $0.6.10^{-4}$ M) (3,4); Sch. 44 (C= $2.10^{-4}$ M) and Sch. 45 (C= $1.2.10^{-4}$ M) (5,6)

This class of novel photoswitchable multicolor fluorescent polymer nanoparticles may find potential applications in multiplexed bioassays.

Conjugated polymer nanoparticles based on poly(9,9-dihexylfluorene-*alt*-2,1,3-benzoxadiazole) as the fluorescent host polymer and photochromic diarylethene

as the toggle for reversible fluorescence photoswitching have been prepared. The precipitation method using 1,2-distearoyl-sn-glycero-3-phosphoethanolamine-N-[amino(polyethylene glycol)-2000] was used [70]. Fluorescence switching was characterized by high contrast of up to 90-fold and recovery efficiency of 95 %.

Effective modulation of a fluorescence switch based on the FRET-effect may be reached for composite nanoparticles based on photochromic compounds and other organic fluorophores [71, 72]. Composite nanoparticles containing photochromic 5-methoxy-1,3,3trimethyl-9'-hydroxyspiroindolinenaphthoxazine, 4-(dicyanomethylene)-2-methyl-6-(p-dimethylaminostyryl)-4H-pyran, and emissive-assistant bis(pyrene)propane in a polyvinyl acetate (PVA) film provide high contrast of the fluorescent signal [71]. Reversible and thermally bistable fluorescence switching occurs in the PVA film with composite nanoparticles based on photochromic (1,2-bis(2-methylbenzo[b]thiophen-3-yl)hexafluorocyclopentene) and fluorescent N,N-di[3-hydroxy-4-(2-benzothiazole)phenyl]-5-tert-butylisophthalamide, which shows an aggregation-induced enhanced emission in the solid state [72].

Different fluorescence properties of photochromic nanoparticles may be embodied with the use of fluorophore–photochrome dyads Sch. 46 [73]. Fluorescent properties of these dyads depend on the structure of the fluorophore fragment (Table 2).

These fluorophore—photochrome dyads with an oligo(ethylene glycol) chain attached to their 2H,3H-indole moiety were used to prepare photoactivatable nanoparticles by their encapsulation within the hydrophobic core of polymer micelles.

One of important steps in fabricating optoelectronic devices is the realization of the metal-organic junctions [74]. A particular interest is aroused by the use of photochromic compounds in these junctions, which allows creation of reversible photoswitches. Unfortunately, polymeric nanoparticles are subject to pH-dependent swelling and agglomeration. Therefore, they lead to linking effects and change their physical properties in different solvents [40, 66, 75].

#### Silica nanoparticles

The method of the synthesis of polymerically derivatized photosensitive colloidal silica nanoparticles was developed, using a spiropyran-co-methacrylate copolymer brush containing 20 mol % of spiropyran units in pendant groups Sch. 43 [76, 77]

The polymers were grown from initiator-functionalized silica nanoparticles by atom-transfer radical polymerization. It was found that, in contrast to analogous polymer solutions, the particulate dispersion viscosity increased on exposure to UV light due to particle aggregation. By appropriate choice of the solvent polarity, it is possible to attain the optimum photoaggregation behavior for polymeric brush with an invariable photochromic content [78].

Spiropyran—methyl methacrylate copolymers Sch. 48 were grafted from flat silica surfaces and colloidal particles utilizing atom transfer radical polymerization [40]. The spectral-kinetic data of thermal bleaching of colloidal particles indicated the presence of free and H-stacked merocyanines in solutions.

In this connection, silica nanoparticles have significant advantages because they are immune to swelling and easy to modify by the Stober method from silyl ether as the precursor in an ammonia solution. This method was used for incorporation of functionalized diarylethene into silica nanoparticles possessing the FRET effect [79]. A new functional (amino reactive) highly efficient fluorescent molecular switch containing photochromic diarylethene Sch. 49 and Rhodamine fluorescent dye Sch. 50 was developed.

The spectroscopic and switching properties of 30 nm size particles in an ethanol suspension were the same as for the photochromic compound in ethanol, except the 5-nm bathochromic shift of the absorption and emission spectra.

Dye-doped core (silica core)-shell nanoparticles capable of reversible photoswitching were prepared with the use of Pluronic F127 direct micelles [80]. The Rodamine B derivative Sch. 51 ( $\varphi^{fl}$  =0.35) was entrapped in the core and the molecules of photochromic diarylethene Sch. 52 were incorporated into the outer shell. The reversible fluorescence quenching mechanism is based on the FRET effect. The energy transfer process from fluorescent dye molecules in the core to the diarylethene derivative hosted in the polyethylene glycol (PEG) shell was realized. As a result, modulation of fluorescence intensity at 590 nm was observed according to photochromic transformations between the open ( $\lambda_A^{max}$  =320 nm) and closed ( $\lambda_B^{max}$  =630 nm) forms.

Similar results were obtained in a study of nanoparticles based on the same Rhodamine B Sch. 51 and functionalized spiropyran Sch. 53 [81]. As shown in Fig. 8, these nanoparticles provide reversible fluorescence modulation without a significant loss of the emission intensity. It was established that the efficiency of fluorescence photoswitching was different depending on the molar ratios of the photochromic compound and the fluorophore, but did

Table 2: Photochemical and photophysical parameters of fluorophore-photochrome diads Sch. 42 in acetonitrile at 20°C.

Compound	$\lambda_A^{max}$ ,nm	$oldsymbol{arphi}_{AB}$	$\iota_B$ ,ms	$\lambda_B^{max}$ ,nm	$\lambda_B^{fl.max}$ ,nm	$oldsymbol{arphi}^{fl}$
1	288	0.08	0.1	412	542	< 0.01
2	299	0.02	0.1	431	559	< 0.01
3	362	-	-	501	630	< 0.01
4	412	0.02	0.2	573	645	0.09
5	548	-	-	543	565	0.03
6	520	-	31	558	-	-

Note:  $\lambda_A^{max}$ ,  $\lambda_B^{max}$ ,  $\lambda_B^{fl.max}$  – maxima of absorption bands of initial, photoinduced forms of diads and a maximum of fluorescent band of the photoinduced form, accordingly;  $\varphi_{AB}$  and  $\varphi^{fl}$  –quantum yields of photocoloration and fluorescence of the photoinduced form, accordingly;  $\iota_B$ - the lifetime of the photoinduced form.

not depend on the size. The fluorescent silica spherical nanoparticles manifesting reversible fluorescence modulation were prepared with the use of a photochromic luminescent steroid-based organogels [42]. The initial composition contained organogel Sch. 54, the tetraphenoxylated perylene diimide Sch. 55 or alkoxy-silane-substituted perylene diimide Sch. 56, and dinito-substituted benzothienylic diarylethene Sch. 57. Fluorescent properties of nanoparticles were provided by application of physically Sch. 55 or chemically Sch. 56 admixed perylene dyes.

Photoswitchable nanoparticles based on photochromic diarylethene and a highly biocompatible photoluminescent fullerene-silica as fluorophore Sch. 58 were prepared by the reverse-microemulsion method [82]. They provide reversible fluorescent modulation in the spectral range of 500-700 nm.

It was found that the photocyclization efficiency of (1,2-bis[2-methylbenzo[b]thiophen-3-yl]-3,3,4,4,5,5 - hexafluoro-1-cyclopentene) increased with decrease in the silica pore diameter in the range of 1.2-3.8 nm [83]. It is explained by increasing concentration of molecules in the rod-like anti-parallel form in the pore structure.

The study of photochromic transformation of 5-chloro-1,3-dihydro-1,3,3-trimethylspiro[2H-indole-2,3'-

(3H)naphta[2,1-b](1,4)oxazine] in functionalized mesoporous silica showed that the rate of thermal bleaching of the photoinduced merocyanine form decreased with increasing concentration of the photochromic compound and decreasing the pore size [84]. An increase in the density of surface silanol groups and the presence of acidic functional groups on the silica walls retard the thermal bleaching of the merocyanine form but basic functional groups reduce the stability of this form.

#### Nanoparticles based on quantum dots

Quantum dots (QDs) may function as efficient FRET donors in photochromic nanoparticles. They posses unique properties, namely non-toxicity, excitability by one or more photons over a wide spectral range, emission in a narrow and programmable spectral range, and photostability.

At the first time, photoinduced fluorescent modulation was demonstrated with the use of photochromic nanoparticles containing photochromic 1',3-dihydro-1'-(2-carboxyethyl)-3,3-dimethyl-6-nitrospiro-[2H-1-benzopyran-2,2'-(2H)-indoline Sch. 59 attached to the QD (CdSe/ZnS semiconductor nanocrystals)-coordinated protein [57]. It is very important for nondestructive readout

Scheme 47

Scheme 48

Scheme 49

Scheme 50

Scheme 51

Scheme 52

of the fluorescence signal that QDs may be excited at any discrete wavelength outside the absorption bands of the closed and open spiropyran forms. Reversible modulation of the fluorescence intensity was reached by using the FRET-effect. The level of nondestructive fluorescence modulation can be adjusted by increasing the number of spiropyran molecules attached to QDs.

Spiropyrans with a dithiolane anchoring substituents were used to prepare photochromic nanoparticles based on QDs [85]. Using spiropyrans with thiol-containing linkers, photochromic CdSe/ZnS nanoparticles were prepared.

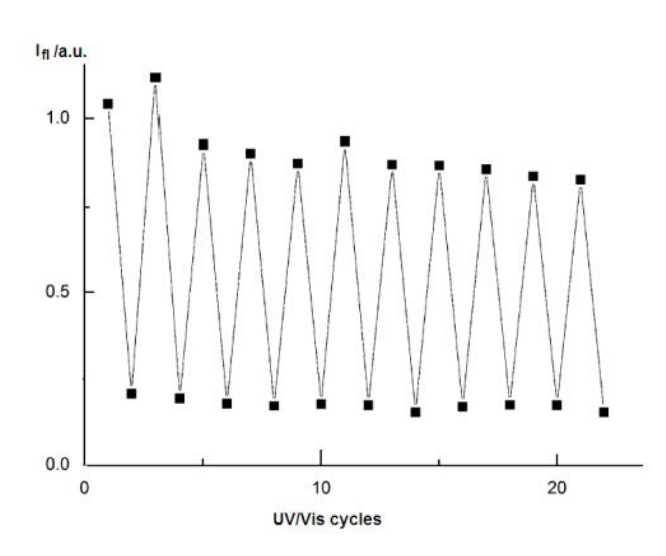


**Figure 8:** Fluorescence intensity switching cycles for photochromic nanoparticles based on Rhodamine B Sch. 51 and functionalized spiropyran Sch. 53 in ethanol ( $C=3.10^{-4}$  M) upon irradiation with UV (350 nm, 30 s) and visible (Vis) light (590 nm, 30 s) exited at 520 nm and recorded at 593 nm.

These photochromic nanoparticles exhibited complete fluorescence quenching in the presence of 80 bound photochromic molecules per particle [86].

Modification of CdSe nanoparticles by functionalized spiropyran using the Cu(I)-mediated "click" reaction provided a more effective decrease in QD fluorescence intensity by the FRET-effect as compared with other methods [75]. This effect is due to the presence of residual Cu(I) ions.

The application of photochromic spiropyran with a dithiolane appendage for the preparation of photocromic ODs based on CdS resulted in photochromic nanoparti-

Scheme 54

Scheme 55

cles manifesting positive or negative photochromism depending on the preparation method [87]. Nanoparticles prepared in the presence of tri-n-octylphosphine showed positive photochromism. Negative photochromism was observed for nanoparticles obtained in the presence of sodium dioctyl sulfosuccinate.

The relative study of spiropyran-containing photochromic nanoparticles with CdSe/ZnS and CdS QDs showed that nanoparticles based on CdSe/ZnS QDs manifested the best (45%) fluorescence quenching efficiency [85].

Photochromic spirooxazine-containing nanoparticles were prepared using CdTe QDs coated with 3-mercaptopropionic acid [88] and the presence of poly(N-isopropylacrylamide) [89].

Unlike spiropyrans, photochromic diarylethenes can be used to prepare photochromic nanoparticles with thermally irreversible fluorescence modulation. Figure 9 shows photoinduced reversible absorption and fluorescence changes for the solid-phase film based on CdSe/ZnS QDs and diarylethene Sch. 60 [90].

Diarylethene was used for the preparation of nanoparticles based on CdSe/ZnS QDs, which were directly modified with a large excess of the photochromic com-

24 — V.A. Barachevsky

#### Scheme 56

pound [91]. In this case, fluorescence switching fatigue and strong quenching by both the open and closed forms are observed. These results are attributable to electron transfer competition with FRET and irreversible reduction of the photochromic compound.

With the goal of increasing the thermal stability of photoinduced form and recurrence of photochromic transformations, photochromic biotinylated diarylethene Sch. 61 was used for the preparation of photochromic QDs based on CdSe/ZnS bearing conjugated streptavidin [56]. The interconversion between the open and closed forms upon irradiation at 365 and 546 nm provided reversible modulation of QD fluorescence.

The synthesized amphiphilic polymer coating for CdSe/ZnS and CdSe/CdS/ZnS QDs containing pendant diarylethenes within the hydrophobic layer provided the optimal conditions for the maximum photoconversion [92, 93].

Photochromic diarylethenes were covalently linked to amphiphilic polymer Sch. 62, which is self-assembled with lipophilic chains surrounding the commercial hy-

Scheme 57

Scheme 58

Scheme 59

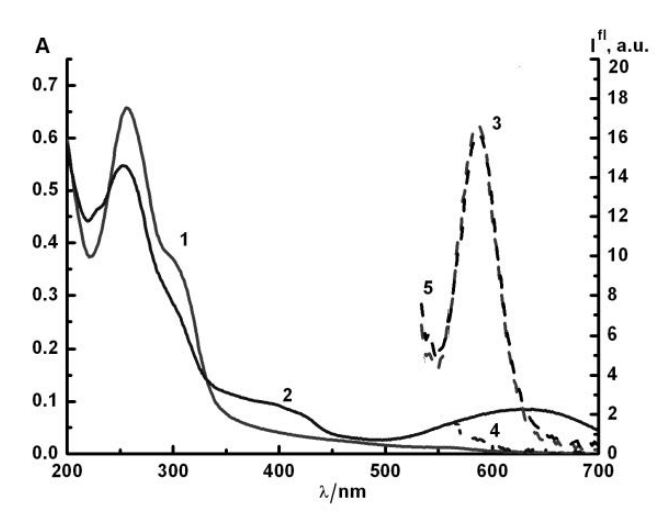


**Figure 9:** Absorption (1,2) and fluorescence (3-5) spectra of the photochromic solid-phase film containing diarylethene Sch. 60 (C=4,7.10 $^{-3}$  M) and CdSe/ZnS quantum dots (1:1 weight ratio) before (1,3) and after UV (2,4) and the subsequent visible (5) irradiation.

Scheme 61

drophobic core–shell CdSe/ZnS QDs [94]. The prepared nanoparticls 7 nm in diameter were soluble in the aqueous medium. The FRET fluorescence modulation monitored by steady-state and time-resolved methods was 35-40%.

The CdSe/CdS/ZnS QDs were used as templates for self-assembling of photoswitchable amphiphilic polymers with a poly[isobutylene-alt-maleic anhydride] backbone and pendant dodecyl alkyl chains, photochromic [2-amino-N-(3,3,4,4,5,5-hexafluoro-2-methylbenzo[b]-thiophen-3-yl)cyclopent-1-enyl)-2-methylbenzo[b]thiophen-6-yl)propanavide with alanine linker Sch. 63 and fluorophore Lucifer Yellow

#### Scheme 62

(LY) Sch. 64 [95]. These nanoparticles 20 nm in diameter show a dual-color emission at 525 and 635 nm.

Scheme 63

Scheme 64

26 **DE GRUYTER** OPEN V.A. Barachevsky

Spectroscopic investigations of the FRET effect by means of systems consisting of CdSe QDs and photochromic dve hybrid Sch. 65 showed photoinduced fluorescence modulation with an efficiency of up to 80 % [96]. It was shown that in the closed form of diarylethene, FRET is the key fluorescence quenching mechanism. Moderate quenching observed for the open isomer is due to non-FRET pathways.

Scheme 65

Nano-biophotonic hybrid systems with the photocontrolled FRET-effect were developed with the use of CdSe/ZnS core-shell QDs and photochromic protein bacteriorhodopsin in its purple membrane [97]. It was shown that electrostatic self-assembling of QDs and purple membranes or (QD-streptavidin)-(purple membrane-biotin) linking give rise to FRET-efficiencies exceeding 80 %.

#### Doped upconversion nanoparticles

Photochromic nanoparticles may be created by combining upconversion nanoparticles containing crystalline NaYF<sub>4</sub> doped with trivalent lanthanide ions [98– 100]. As a fluopophore, monodisperse rare-earthdoped upconversion nanophosphors  $\beta$ -NaYF<sub>4</sub>:Yb,Er  $(\lambda_n^{max})$  =540 and 650 nm) were used together with photochromic 1-{4(5-methoxy-2-(2-pyridyl)thiazolyl)}-2-{3-(2methylbenzo[b]thiophenyl)}hexafluorocyclopentene Sch. 66 sive structures [99]. The spectral and fluorescence charac- $(\lambda_A^{max} = 325 \text{ nm}, \lambda_B^{max} = 550 \text{ nm})$  [98]. Figure 10 shows that these nanoparticles are characterized by absorption spectra of photochromic diarylethene and the fluorescence spectrum providing reversible FRET fluorescence quenching.

Nondestructive readout of fluorescence modulation was achieved upon near-IR excitation ( $\lambda = 900$  nm). This system was used to manufacture a recording medium for rewritable optical storage with nondestructive readout.

Scheme 66

$$R_{2} = -CH_{3}$$

$$R_{3} = -CH_{3}$$

$$R_{4} = -CH_{3}$$

$$R_{2} = -CH_{3}$$

$$R_{2} = -CH_{3}$$

$$R_{2} = -CH_{3}$$

$$R_{3} = -CH_{3}$$

$$R_{4} = -CH_{3}$$

$$R_{2} = -CH_{3}$$

$$R_{2} = -CH_{3}$$

$$R_{3} = -CH_{3}$$

$$R_{4} = -CH_{3}$$

$$R_{2} = -CH_{3}$$

$$R_{2} = -CH_{3}$$

$$R_{2} = -CH_{3}$$

$$R_{3} = -CH_{3}$$

$$R_{4} = -CH_{3}$$

$$R_{2} = -CH_{3}$$

$$R_{2} = -CH_{3}$$

$$R_{3} = -CH_{3}$$

$$R_{4} = -CH_{3}$$

$$R_{4} = -CH_{3}$$

$$R_{5} = -CH_{3}$$

$$R_{7} = -CH_{3}$$

$$R_{7} = -CH_{3}$$

$$R_{7} = -CH_{3}$$

$$R_{8} = -CH_{3}$$

$$R_{1} = -CH_{3}$$

$$R_{2} = -CH_{3}$$

$$R_{2} = -CH_{3}$$

$$R_{2} = -CH_{3}$$

$$R_{3} = -CH_{3}$$

$$R_{4} = -CH_{3}$$

$$R_{5} = -CH_{3}$$

$$R_{5} = -CH_{3}$$

$$R_{7} = -CH_{3}$$

$$R_{7} = -CH_{3}$$

$$R_{7} = -CH_{3}$$

$$R_{8} = -CH_{3}$$

$$R_{1} = -CH_{3}$$

$$R_{2} = -CH_{3}$$

$$R_{2} = -CH_{3}$$

$$R_{2} = -CH_{3}$$

$$R_{3} = -CH_{3}$$

$$R_{4} = -CH_{3}$$

$$R_{5} = -CH_{3}$$

$$R_{7} = -CH_{3}$$

$$R_{8} = -CH_{3}$$

$$R_{1} = -CH_{3}$$

$$R_{2} = -CH_{3}$$

$$R_{2} = -CH_{3}$$

$$R_{3} = -CH_{3}$$

$$R_{4} = -CH_{3}$$

$$R_{5} = -CH_{3}$$

$$R_{7} = -CH_{3}$$

$$R_{8} = -CH_{3}$$

$$R_{1} = -CH_{3}$$

$$R_{2} = -CH_{3}$$

$$R_{2} = -CH_{3}$$

$$R_{3} = -CH_{3}$$

$$R_{4} = -CH_{3}$$

$$R_{5} = -CH_{3}$$

$$R_{7} = -CH_{3}$$

$$R_{8} = -CH_{3}$$

$$R_{8} = -CH_{8}$$

$$R_{1} = -CH_{1}$$

$$R_{2} = -CH_{3}$$

$$R_{3} = -CH_{1}$$

$$R_{4} = -CH_{1}$$

$$R_{5} = -CH_{1}$$

$$R_{7} = -CH_{1}$$

$$R_{8} = -CH_{1}$$

$$R_{1} = -CH_{1}$$

$$R_{2} = -CH_{1}$$

$$R_{3} = -CH_{1}$$

$$R_{4} = -CH_{1}$$

$$R_{5} = -CH_{1}$$

$$R_{7} = -CH_{1}$$

$$R_{8} = -CH_{1}$$

$$R_{1} = -C$$

Scheme 67

Scheme 68

Water-soluble encapsulated upconversion nanoparticles based on a number of diarylethenes Sch. 67 and Sch. 68 and lanthanides were prepared by treating a CHCl3 solution of oleate-coated nanocrystals with poly(styrene-co-maleic anhydride) followed by sequential addition of poly(propylene glycol)bis-(2-aminopropyl ether) and one of diarylethenes. After stirring, the organic solvent was replaced with water, which gave rise to aqueous dispersions of the self-assembled photoresponteristics of these nanopartices depend on the structure of photochromic compounds.

Hybrid nanoparticles containing NaYF4:ErYb and diarylethene Sch. 69 with the alkyne group necessary for "click" chemistry and a methoxypolyethylene glycol chain providing water dispersibility and eventual biocompatibility were used for photomodulation of green fluorescence  $(\lambda = 510 - 560 \text{ nm})$  in living organisms [100].

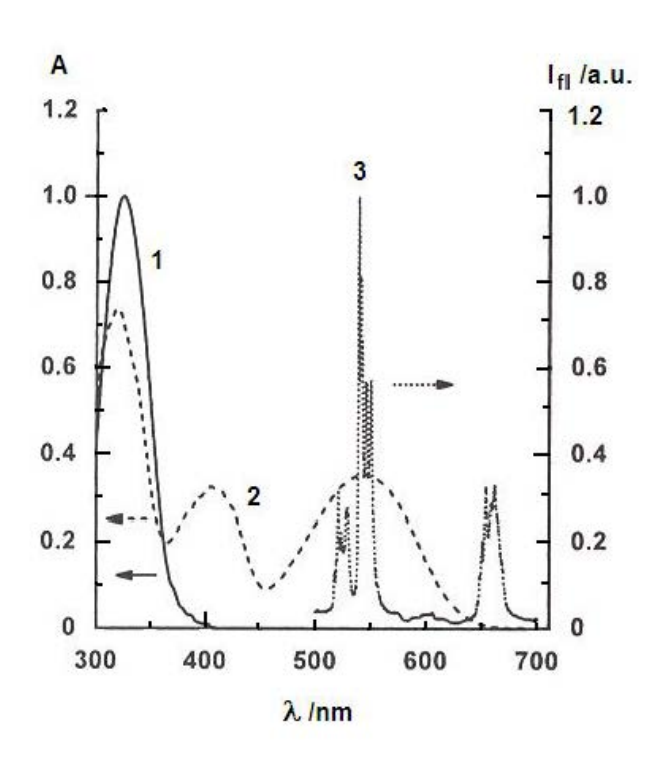


**Figure 10:** Absorption spectra of open A (1) and closed B (2) forms of diarylethene Sch. 66 and the emission spectrum of upconversion nanoparticles NaYF<sub>4</sub>: Yb, Er deposited on a silicon wafer in acetonitrile.

Scheme 70

The new diarylethene derivative Sch. 70 was used to prepare upconversion nanoparticles based on NaYF<sub>4</sub>:TmYb [101].

The photoswitching of near-infrared excited upconversion nanoparticles based on LiYF<sub>4</sub>:Tm,Yb was demonstrated with the use of bis-spiropyran [102].

Light-controlled reverse Pickering emulsions based on upconversion nanophosphors NaYF<sub>4</sub>:Yb and carboxylcontaining spiropyran were used for enantioselective biocatalysis in biphasic systems [103]. A reversible inversion of the properties of Pickering emulsions is provided by photochromic transformations upon alternating UV fluorescence of nanophosphors excited by multiphoton irradiation and visible light.

A hybrid nanostructure comprising dual-emissive rare-earth upconversion nanophosphors and a photochromic spiropyran demontrated reversible switching of the green emission of nanoparticles [104]. The covalent grafting guarantees a high efficiency of the energy transfer, a relatively large on/off ratio, and good durability.

Today studies of photochrmic nanoparticles deal with the development of multimodal fluorescence modulation (chameleon nanoparticles) [67, 69, 105]. In the case of upconversion nanoparticles, it is achieved by application of two photochromic diarylethenes possessing different photoinduced absorption. These compounds provide the emission change using the FRET effect between photoinduced isomers of diarylethenes Sch. 71 and upconversion nanoparticles  $\beta$ NaYF<sub>4</sub>:Tm,Yb,Er [105].

Photochromic transformations of diarylethene Sch. 72 were demonstrated using two types of photon upconversion nanoparticles NaYF<sub>4</sub>:TmYb (UV irradiation) and NaYF<sub>4</sub>:ErYb (visible irradiation) [106]. It showed a "remote control" photorelease with diarylethene of an unusual structure.

Scheme 71

$$\begin{array}{c} \text{CO}_2\text{Et}_{\text{CN}} \\ \text{R} \\ \text{EtO}_2\text{C} \\ \text{R} \\ \text{Visible} \\ \text{R} \\ \text{R} \\ \text{C}_{11} \\ \text{H}_{22} \\ \end{array}$$

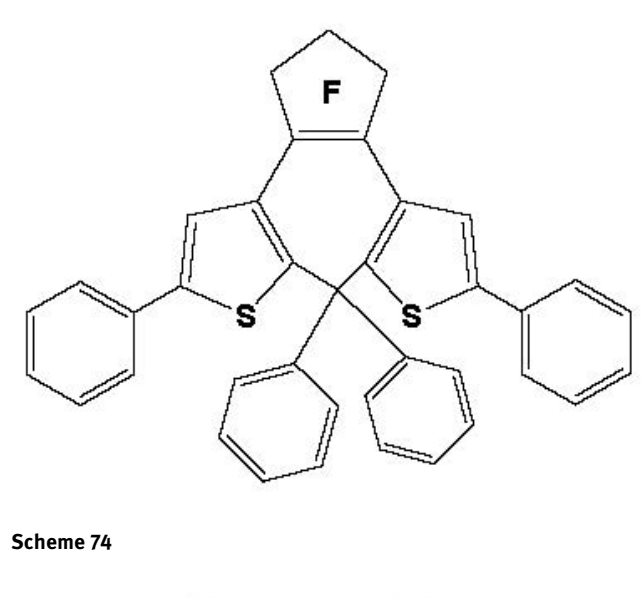
#### Scheme 72

Photochromic transformations of diaylethenes Sch. 73 and Sch. 74 in colloidal solutions containing NaYF<sub>4</sub> nanoparticles doped by Er<sup>3+</sup>/Yb<sup>3+</sup> and Tm<sup>3+</sup>/Yb<sup>3+</sup> ions were induced only by intensity of the near-infrared light (980 nm) (Fig. 11) [107]. The key aspect is nonlinearity of the upconversion mechanism providing selective generation of UV and blue light under high-power conditions for photochromic transformations.

Scheme 73

Photoswitchable polymer nanoparticles have been constructed by emulsion polymerization iridium(III) through embedding an complex, [Ir(phenylbenzothiazole)<sub>2</sub>(picolinate)] as a fluorophore and a diarylethene derivative as a photochrome [108].

A novel and unique method for highly efficient fluorescence photoswitching utilizing photochromic diarylethene and upconversion LaF<sub>3</sub>:Yb,Ho nanophosphors ( $\lambda_{max}^{fl}$  =540 nm) was suggested [109].



higher power NIR 980 nm

UV

VIS

lower power NIR 980 nm

decreasing IR power

tunable upconversion

upconversion nanoparticle

Figure 11: Scheme of diarylethene photochromic transformations under NIR (980 nm) irradiation of different power

#### Ag - Nanoparticles

A number of papers are devoted to photochromism of diaryethenes on the surface of the silver (Ag) nanoparticles. The study of photochromism of Ag-nanopatricles covered with diarylethene containing an anthracene unit Sch. 75 showed the conversion from the open to closed isomer to decrease from 81 to 16 % [110]. Fluorescence from the anthracene unit of the open isomer ( $\varphi^{fl}=$ 0.009) was quenched to 7.6 % of the unbound state. This effect is related to the exited energy transfer from diarylethene

molecules to the Ag nanoparticles and to overlap of the fluorescence band of diarylethene and the plasmon absorption band of Ag-nanoparticles. The cycloreversion reaction was scarcely affected.

Scheme 75

#### Scheme 76

The Ag nanoparticles covered with photochromic diarylethene polymers Sch. 76 manifest the effect of plasmonic enhancement on the photochromic transformations [111]. It was found that the photocycloreversion reaction is enhanced by an order of magnitude under visible light. This phenomenon is due to electromagnetic field enhancement near the surface of the silver core.

Derivatives of photochromic compounds with thiol groups are often used for realization of effective molecular interaction of photochromic compounds, in particulary diarylethenes, with nanoparticles of precious metals. The synthesis of these compounds presents certain difficulties. In this connection, for the first time, novel photochromic thiosemicarbazide and thiocarbazate derivatives of dithienylperfluorocyclopentenes Sch. 77 were synthesized [112].

 $R = NH_2$ , NHPh,  $4-MeC_6H_4NH$ ,  $2-MeC_6H_4NH$ ,  $4-FC_6H_4NH$ ,  $2-FC_6H_4NH$ , SMe

#### Scheme 77

The chemical reaction between Ag nanoparticles and these diarylethenes was detected by the spectral-kinetic method [113]. It is manu\ifested as spectral variations, including the variation of intensity and structure of absorption bands as well as in the significant bathochromic shift for the absorption band of the photoinduced cyclic form (Fig. 12). This is supported by kinetic changes in the photocoloration and photobleaching processes. The presence of Ag nanoparticles in solution increases the stability of photochromic diarylethenes to irreversible phototransformations. Disappearance of photochromism at the presence

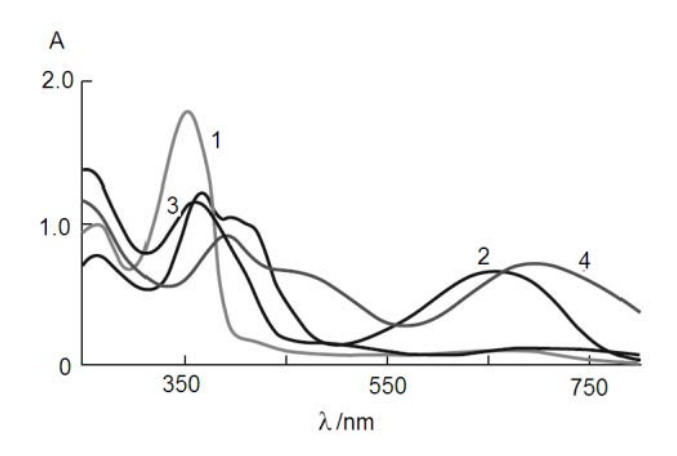


**Figure 12:** Absorption spectra of compound Sch. 77(R=NHPh) in dimethyl sulfoxide without (1,2) or in the presence (3,4) of Agnanoparticles before (1,3) and after (2,4) UV irradiation.

of Ag nanoparticles was found for spiropyran Sch. 78 [114].

Scheme 78

Scheme 79

A reversible strong coupling was found between dipolar surface plasmon resonance of Ag nanoparticles and the electronic transition of spiropyran molecules in a polymer binder [115]. The coupling strength depended on the spectral position of the surface plasmon resonance and the conformational molecular state. It is possible if the molecular transition and plasmon resonance are closely matched.

The comparative spectral-kinetic research of photochromism of unsubstituted spirooxazine Sch. 79.1 and its analogue Sch. 79.2, containing the thiol group, showed that unlike the former compound, molecules of compound Sch. 79.2 experience strong chemical interaction with Ag nanoparticles [114]. Thiss is indicated by the bathochromic spectral shift of the absorption band of the photoinduced form, decrease in the rate constant of spontaneous bleaching of the photoinduced merocyanine form, and increase in the stability of photochromic molecules connected with Ag nanoparticles to irreversible phototransformations.

Excitation of localized surface plasmons between Ag nanoparticles (nanospheres, nanoprisms, nanowires, nanodisks) enhances the photochromic efficiency of photochromic chromene, namely, 3-bromo-2,2-dimethyl-2H-pyrano[3,2-c]chromen-5-one [116].

Novel photochromic thiol-terminated 1,3-diazabicyclo[3.1.0]hex-3-enes Sch. 80 and Sch. 81 were used for the preparation photochromic Ag nanoparticles [117, 118]. It was established that there is chemical interaction between Ag nanoparticles and the terminal thiol groups of photochromic compounds [118]. Compounds with disulfide bonds showed a pronounced bathochromic spectral shift of the absorption band of the open-ring isomer and also in the surface plasmon resonance absorption of the photochromic nanoparticles [117].

Scheme 80

Scheme 81

It was found that an Ag film prepared by vapor deposition on an organic photochromic diarylethene consisted of small Ag nanocrystals [119]. The resistance of such a film

was reduced 10<sup>6</sup>-fold after UV irradiation and was restored on explosure to visible light.

#### 2.2.1 Au nanoparticles

Photochromic nanoparticles based on gold (Au) nanoparticles and S-H functionalized spiropyran Sch. 82 may be used to design photocontrolled release drug delivery systems [120]. The specific binding properties of these photochromic nanoparticles, for example, reactions with amino acids, open up prospects for their application in biological studies.

Scheme 82

Scheme 83

Photochromic 6-nitro-substituted spiropyran modified with a disulfide-terminated aliphatic chain Sch. 83

was used for preparing photochromic Au-nanorods *via* the strong covalent S-Au bond [121]. These nanoparticles were very stable in organic solvents without any aggregations or decomposition. This modified photochromic 6-nitrospyropyran prepared on polycrystalline Au surfaces manifests excellent reversible electrochemical properties [122].

Photochromic spiropyrans may be used for preparation of photoinduced aggregation systems [123, 124]. Sulfur-containing spiropyran Sch. 84 was used for irreversible self-aggregation of Au nanoparticles [123]. This compound exists in the spirocyclic form which scarcely associates with nanoparticles. The photoinduced merocyanine form of this spiropyran is covalently bonded to the surface nanoparticles by its thiolate moiety. This change triggers the aggregation.

$$\begin{array}{c|c} hv_1 \\ \hline \\ hv_2, kT \end{array}$$

Scheme 84

Scheme 85

The mechanism of this aggregation is explained by surface properties of Au-nanoparticles. In aqueous solutions, the surface is covered by negatively charged carboxylic acid groups (-COO<sup>-</sup>). In the dark, Au nanoparticles are dispersed owing to electrostatic repulsion. After UV irradiation, the positive charge on the indole moiety of the adsorbed merocyanine form neutralizes the negative charge of the surface carboxyl groups. This decreases the electrostatic repulsion between Au-nanoparticles and triggers its aggregation. It was demonstrated that unlike solutions, the photoinduced merocyanine form does not transform into the initial spiropyran isomer under visible light. In this connection, thiol-terminated spiropyran of another type Sch. 85 was used for modification of Au-nanoparticles [124]. In this case, photocontrolled reversible aggregation of Au-nanoparticles (5 nm) giving aggregates of the 20-340 nm size and narrow size distributions (standart deviation < 34 %) was observed. These aggregates retain their size in the dark because of the thermal reverse isomerization is suppressed due to stacking interaction between the merocyanine molecules. The mechanism of reversible repulsion/attraction between nanoparticles is related to ring opening/ring closure photoisomerization of the surface photochromic compounds.

The extinction spectra of J-aggregated dyes on Au nanopatricles which exhibit interferences between the plasmon and dye resonances were simulated using a quantum mechanical model [125]. According to this model, the dye transition interacts with the continuum of nanoparticle states through transition-dipole coupling.

A study of the fluorescent properties of the system based on photochromic 1,3,3- trimethyl-6-nitrospiro-[2H-1-benzopyran-2,2'-indoline and Au nanoparticles showed a significant increase in the emissive brightness of the photoinduced merocyanine form [126].

Photocontrolled Au spyropyran nanoparticles were used for the development of resettable multi-readout logic gates [127].

As in case of Ag nanoparticles [110], a decrease in the conversion from the open to closed isomer was found for the systems based on Au nanoparticles with the use of photochromic compounds which were separated from the metal core by alkyl chain [128, 129]. These experimental results were supported by the theoretical study of the electronic and optical properties of photochromic dithienylethene derivatives connected to small gold clusters [130].

The study of diarylethene molecules with an anchoring sulfur atom connected to the Au nanoparticles via an aromatic spacer showed that their photochromism depends on the nature of the spacer [131]. It was found that, contrary to diarylethenes Sch. 86 and Sch. 87, compound Sch. 88 shows no photochromic transformations at the presence of the Au nanoparticles.

Scheme 86

Scheme 87

Scheme 88

A related study of symmetric and asymmetric diarylethenes Sch. 89 - Sch. 91 immobilized on Au nanoparticles demonstrated that the asymmetric diarylethenes display a higher thermal barrier to ring opening than symmetric analogs and their photochemical ring-closure is inhibited by gold [132].

Scheme 89

The Au nanoparticles coated with photochromic dyarylethene polymers or block copolymers Sch. 92 were prepared according to the Brust's method for evaluation of the electric field interaction between the Au nanoparticle and photochromic diarylethene moieties [133]. It was found that the photochromic photocyclization reactivity decreases upon shortening of the distance between the Au surface and the diarylethene moiety. Thus, a bathochromic spectral shift in the absorption maximum

Scheme 90

Scheme 91

of the diarylethene closed form was observed. This shift is connected with the local electric field generated by the surface plasmon resonance of Au nanoparticles. The position of the absorption band of the local surface plasmon resonance strongly depends on the size of the Au particles [134]. The photocycloreversible reaction is enhanced in the vicinity of the Au nanoparticle [135].

Compounds Sch. 93 - Sch. 96 have been synthesized for the following study of the effect of diarylethene monomers with various diarylethene fragments in the side chain [136]. It was established that structural differences of photochromic fragments had no effect on the degree of enhancement [137].

The synthetic procedure for preparation of photochromic Au nanoparticles of different sizes (13 and 41 nm) coated with polystyrene using organic acid salts and ligand exchange reaction was developed. The larger Au particles were obtained using disodium malate instead of citrate [138]. The use of thermo- and photoresponsive poly(N-isopropylacrylamide) resulted in Au nanoparticles which exhibited a bathochromic spectral shift in solution upon heating or UV irradiation [139].

Two-photon bleaching of the diarylethene closed isomer in the ultrathin polymer film coated onto the Aunanoparticle-integrated glass substrate under NIR-CW laser radiation ( $\lambda = 808$  nm) was found [140]. The pho-

Scheme 92

Scheme 93

Scheme 94

tochromic compound receives energy from two photons which excite the state favorable for bleaching the diarylethene closed form enhanced by localized surface plasmon. Enhancement of two-photon bleaching of the diaryethene closed isomer is observed in solutions of

Scheme 95

Scheme 96

Au nanodimer structures [141]. The NIR ring opening of the diarylethene closed form was observed during a study of Au nanoparticles by surface-enhanced Raman scattering [142]. Two-photon bleaching of the closed form of 1,2-bis(2,4-dimethyl-5-phenyl-3-thienyl)-3,3,4,4,5,5-hexafluoro-1-cyclopentene was implemented by using incoherent NIR light irradiation instead of laser for the Au nanoparticle 2D array on the conductive layer of indiumtin-oxide (ITO) [143].

A study of photochromic transformations of diarylethenes into hybrid thin films showed the acceleration of the ring-opening photochemical reaction in the presence of Au nanoparticles [144].

Azobenzene- and stilbene-terminated alkanethiolate molecules [145] as well as unsymmetrical azobenzene disulfide Sch. 97 were used for functionalization of Au nanoparticles [146]. The *trans*-to-*cis* photoisomerization of the appended compounds was observed in solutions and in the composite clusters. The quantum yields of photopolymerization of the composite clusters was affected by the length of the linker because of different quenching photoisomerization by the metal core. According to FTIR spectra of azobenzene disulfide captured by Au nanoparticles (5 nm) showed that molecules are in the all–*trans* conformation. The photoinduced reaction rates follow first-order kinetics and are identical to those of free azobenzene molecules. This suggests that

no any steric effects are involved in the reactions. A Raman spectroscopy study of the *cis-trans* photoconversion of 4-dimethylamino-azobenzenecarbocxylate on the Aunanoparticle surface indicated that both the *cis-* and *trans*-conformations coexist after adsorption [147]. Irradiation of functionalized Au-nanoparticles by 440 nm light decreased the concentration of molecules in the *cis-*form.

$$C_6H_{13}$$
  $N$   $N$   $O-C_{12}H_{24}$   $S-S-C_{12}H_{25}$ 

Scheme 97

Scheme 98

The Au nanoparticles having a monolayer of azobenzene liquid crystal Sch. 99 of the 4.7 nm diameter undergo photochemical and thermal isomerization by analogy with free azobenzenes in solution [148]. However, self-organization of molecules on the surface of nanoparticles is observed because of crystallinity of the organic ligands attached to the surface.

Photoswitching in self-assemled monolayer of azobenzene Sch. 99 capped on ZnO was demonstrated [149]. The extent of packing and efficiency of photochromic switching depended on the shape of nanoparticles. They are less effective in the case of nanorods than nanodots.

Scheme 99

Azodyes were used for the preparation of nanoparticles based on a cubic siloxane cage (polyhedral oligosilsequioxane) of the Si-O skeleton surrounded by covalently attached eight groups of azobenzene mesogens Sch. 100 [150]. These nanoparticles and nematic liq-

$$-(H_2C)_3$$
  $N$   $N$   $O$   $CH$   $CH_2$ 

Scheme 100

uid crystals provide new materials with photocontrolled nonlinear properties.

Unlike the analog with a thiophene linker [151] metaphenyl-linked diarylethene of this type exhibits light-controlled reversible conduction on the gold surface [152]. Using independent optical control experiments, a one-to-one relationship between molecular photoisomerization and conduction switching was revealed [153]. A photoswitching of the conduction of diarylethene—Au nanoparticle network [154] and switching of the tunneling current of a single diarylethene molecule on the gold surface [155] were demonstrated.

#### Other nanoparticles

At the first time, core/shell organic nanocable constructed with photochromic 1-[2-methyl-5-phenyl-3-thienyl]-2-[2-methyl-5-(p(methyl)phenyl)-3-thienyl]-hexafluorocyclopentene Sch. 101 and coronene Sch. 102 were prepared [156]. This nanocable exhibits not only reversible absorption transformations but reversible electrical conduction and fluorescent switching of the semiconducting coronene. This approach opens up prospects for creation of new photochromic memory devices with nondestructive electrical readout of optical information.

Scheme 101

Photochromic 1,3,3-1'-(1-hydroxyethyl)-3,3'-dimethyl-6-nitro-spiro[2H-1-benzopyran-2,2-indoline] [157] and

Scheme 102

diarylethene [158] were covalently attached to the surface of nanotubes for photocontrolling the conductivity of semiconducting single-wall carbon nanotubes. Photoconductive nanotubes coated by self-assembled diarylethene Sch. 103, appended hexa-peri-hexabenzocoronene Sch. 104, may be modulated by reversible photochemical izomerization of the pendant [159]. The theoretical study using Green's function method combined with density functional theory showed that conductivities of two isomeric diarylethene forms in nanowires differ by a factor of several hundreds [160]. The main contribution to this difference is due to different molecular geometries and  $\pi$ -electron conjugation.

Scheme 103

The non-covalent functionalization of carbon nanotubes with pyrene spiropyran-based dyads containing spacers of different lengths was performed [161]. It was found that in the case of the shorter spacer, the fluorescence band and the absorption band of the photoinduced

$$\begin{array}{c} C_{12}H_{25} \\ \\ C_{12}H_{25} \end{array}$$

Scheme 104

merocyanine form were red-shifted. As this took place, the rate of thermal bleaching of the photoinduced merocyanine form decreased. A combined theoretical and experimental study of the exciton absorption of spiropyran-functionalized carbon nanotubes showed that experimental data are in good qualitative accordance with the theoretically predicted results [162].

Photochromic spiropyran Sch. 59 was used for the development of photoreconfigurable bionanotubes acceptable for guest delivery in the desired time and space domains [163].

Two diarylethenes Sch. 105 and Sch. 106 functionalized with carboxylic groups and grafted onto the surface of ZnO nanorods manifest photochromic transformations under alternating irradiation at 300 and 500 nm [164]. The compound containing a terminal phenyl fragment was characterized by a red-shifted absorption band and better photostability.

Scheme 105

A photocontrolled and quasi-reversible flurescence switch was prepared with the use of hexadecylaminecoated ZnO nanocrystals and diarylethene Sch. 107 [165]. It was establised that diarylethene molecules are weakly

Scheme 106

Scheme 107

adsorbed on the surface of ZnO nanocrystals through hydrogen bonds. Both open and closed diarylethene forms quench the emission of nanoparticles. Quenching occurs mainly through FRET-effect with participation of the closed form. However, the photoinduced electron transfer also occurs for the open form.

At the first time, polyoxotungstate nanocrystals with the molecules of photochromic spiropyrans Sch. 108 and Sch. 109 covalently linked *via* Sonogashira grafting have been elaborated [166]. It was established that grafting of spiropyrans onto polyoxotungstate nanocrystals does not alter significantly the photochromism in solution. Unlike spiropyran crystalline films, solid layers of hybrid compounds display high photochromism depending on the nature and the number of grafted spiropyran groups.

A study of the reaction between diarylethene molecules with a tripodal linker or a carboxyl group and the  ${\rm TiO_2}$  surface by ultrafast absorption spectroscopy showed the absence of electron transfer from the photoexcited tripodal chromophore to  ${\rm TiO_2}$  nanoparticles because

Scheme 109

of the absence of the coupled system [167]. This electron transfer is observed with low efficiency only in the COOH-diarylethene/ ${\rm TiO_2}$  coupled system. It is due to the fast intramolecular relaxation process.

Incorporation of organic photochromes into magnetic systems provides new ways to the development of photocontrolled magnetic nanomaterials [168]. N-Methylated pyridospiropyran Sch. 110 inserted into MnPS $_3$  bye ion exchange to yield Mn $_{1-x}(PS_3)$ (spiropyran) intercalates exhibited photochromism but thermal bleaching reaction was very slow. This strong stabilization of the merocyanine form may be due to the formation of J-aggregates. One of spiropyrans Sch. 104 (R = methyl) acquired a spontaneous magnetization below 40 K, which considerably changed the hysteresis loop under UV irradiation.

Scheme 110

Scheme 111

R=C3H7 or CH3

#### Scheme 112

Photochromic nanoparticles of this type (10-20 nm) were prepared by microemulsion procedure in cyclohexane using polyoxyethylene-oleyl ether [169]. The same method was used to prepare hybrid nanoparticles based on cationic diarylethene Sch. 111 and MnPS<sub>3</sub> [170]. These nanoparticles exhibited typical photochromic and fluorescent reversible switching similar to that for pure diarylethne in solution, but its photoresponse was less sensitive.

The photocontrolled switching of the fluorescence and flocculation displays a new bifunctional nanosystems prepared by encapsulation of sulfur-oxidized diarylethene Sch. 112 molecules onto iron oxide nanoparticles [171]. They showed photoinduced reversible magnetization and demagnetization during the measurement of field dependent magnetization at 300 K.

The increase in the Curie temperature by photoisomerization of diarylethene from  $T_c = 9$  K up to  $T_c = 20$  K was found for organic-inorganic systems based on the 2,2'-dimethyl-3,3'-(perfluorocyclopentene-1,2-diyl)bis(benzo[b]thiophene-6-sulfonate diarylethene

anion Sch. 113 and  $\text{Co}_4(\text{OH})_3(\text{CH}_3\text{COO})\cdot\text{H}_2\text{O}$  by the anion exchange reaction [172]. This enhancement is attributed to the delocalization of  $\pi$ -electrons in the closed form of diarylethene increasing the interlayer interaction.

Scheme 113

## 3 Conclusions

From the beginning of this century a new direction of photochromism, namely, nanophotochromism which includes a development of preparation methods, research into the properties and applications of photochromic nanoparticles has been in progress.

By the present time some preparation methods of photochromic nanoparticles have been developed. Basically, methods of reprecipitation and laser ablation of photochromic substances are used. The greatest attention is given to the development of photochromic nanoparticles of the core-shell type in which polymers, oxides (especially SiO<sub>2</sub>), quantum dots (semi-conductor crystals), nanoparticles of laser crystals and precious metals (Ag, Au) are used as a core. The shell contains thermally reversible (spiropyrans, spirooxazines, chromenes, azo dyes, etc.) or thermally irreversible (diarylethenes, fulgides, etc.) photochromic compounds.

The lines of fundamental research are defined, basically, possible applications of photochromic nanoparticles are outlined. Now two distinct applications, namely, fluorescence labels for biology and medicine and fluorescence photoswitches for optical memory and integrated optics, have been identified. In this connection, systems with the photocontrolled fluorescence working on the basis of the FRET-effect, are extremely demanded. As a result of research, photochromic nanoparticles which provide visualization of the images obtained in biological studies were elaborated. The possibility of application of photochromic nanoparticles in the development of recording media for optical memory was shown.

**Acknowledgement:** This work was supported by the Russian Foundation for Basic Research (projects N 13-03-00964 and N14-03-90022).

### References

- [1] K. Matsuda, M. Irie., J. Photochem. Photobiol. C, 5, 169 (2004).
- [2] C. Yun, J. You, J. Kim, J. Huh, E. Kim., J. Photochem. Photobiol. C, 10, 111 (2009).
- [3] I. Yildiz, E. Deniz, F. M. Raymo., Chem. Soc. Rev., 38, 1859 (2009).
- [4] M. S. Wang, G. Xu, Z. J. Zhang, G. C. Guo., Chem. Commun., 46, 361 (2010).
- [5] M. M. Russew, S. Hecht., Adv. Mater., 22, 3348 (2010).
- [6] T. Fukaminato., J. Photochem. Photobiol. C, 12, 177 (2011).
- [7] T. Nakanishi, K. Matsuda, K. Higashiguchi. In: Supramolecular Soft Matter: Applications in Materials and Organic Electronics, Ed. T. Nakanishi, 2011, Chapter 11.
- [8] E. Harbron. In: Photochemistry, 39, 211 (2011).
- [9] D. Tan, S. Zhou, J. Qiu, N. Khusro., J. Photochem. Photobiol. C, 17, 50 (2011).
- [10] G. Chen, F. Song, X. Xiong, X. Peng., Ind. Eng. Chem. Res., 52, 11228 (2013).
- [11] J. Zhang, Q. Zou, H. Tian., Adv. Mater. 25, 378 (2013).
- [12] T. Feczko, B. Voncina., Current Organic Chemistry, 17, 1771 (2013).
- [13] W. R. Algar, H. Kim, I. L. Medintz, N. Hildebrant., Coord. Chem. Rev., 263-264, 65 (2014).
- [14] V. A. Barachevskii, R. E. Karpov., High Energy Chem., 41, 188 (2007).
- [15] J. Hibino, T. Hashida, M. A. Suzuki, Y. Kishimoto, K. Kanai, Mol. Cryst. Liq. Cryst. Sci. Techn. Section A, 255, 243 (1994).
- [16] Z. Z. Gu, S. Hayami, Q. B. Meng, T. Iyoda, A. Fujushime, O. Sato, J. Am. Chem. Soc., 122, 10730 (2000).
- [17] V. A. Barachevsky, R. E. Karpov, I. A. Nagovitsin, G. K. Chudinova, Yu. P. Strokach, V. S. Miroshnikov, T. A. Chibisova, V. F. Traven', Superlattices and Microstructures, 36, 73 (2004).
- [18] Z. Chen, C. Zhong, Z. Zhang, Z. Li, L. Niu, Y. Bin, F. Zhang, J. Phys. Chem., 112, 7387(2008).
- [19] S. J. Lim, B. K. An, S. D. Jung, M. A. Chung, S. Y. Park, Angew. Chem. Int. Ed., 43, 6346 (2004).
- [20] C. Li, W. L. Gong, Z. Hu, M. P. Aldred, G. F. Zhang, T. Chen, Z. L. Huang, M. Q. Zhu. RSC Adv., 3, 8967 (2013).
- [21] T. Tamaki, M. Sakuragi, K. Ichimura, K. Aoki, I. Arima, Polymer Bull., 24, 559 (1990)
- [22] Q. Sui, J. Zhou. W. He, Z. Li, Y. Wang, Sci. China B, 42, 113 (1990).
- [23] S. Iyengar, M. C. Biewer, Chem. Commun., 1398 (2002).
- [24] S. Iyengar, M. C. Biewer, Cryst. Growth & Design, 5, 2043 (2005).
- [25] T. Mizokuro, H. Mochizuki, M. Xiaoliang, S. Horiuchi, N. Tanaka, N. Tanigaki, T. Hirada, Jpn. Appl. Phys., 42, L983 (2003).
- [26] M. Takeshita, C. N. Choi, M. Irie, Chem. Commun., 2265 (1997).
- [27] M. Takeshita, N. Cato, S. Kawauchi, T. Imase, J. Watanabe, M. Irie, J. Org. Chem., 63, 9306 (1998).
- [28] M. Takeshita, M. Irie, Tetrahedron Lett., 40, 1345 (1999).
- [29] M. Takeshita, M. Yamada, N. Kato, M. Irie, Perkin 2, 619 (2000).

DE GRUYTER OPEN Nanophotochromism — 39

- [30] M. Yamada, M. Takeshita, M. Irie, Mol. Cryst. Liq. Cryst., 345, 431 (2000).
- [31] H. Y. Hu, Z. P. Zhang, X. M. Meng, M. Z. Zhu, Q. X. Guo, Chin. J. Chem. Phys., 20, 103 (2007).
- [32] A. Spangenberg, A. Brosseau, R. Metivier, M. Sliva, K. Nakatani, T. Asahi, T. Uwada, J. Phys. Org. Chem., 20, 985 (2007).
- [33] J. Chen, B. A. Teply, I. Sherifi, J. Sung, G. Luter, F. X. Gu, E. Levy-Nissenbaum, A. F. Radovic-Moreno, R. Langer, O. C. Farokhzad, Biomaterials, 28,869 (2007).
- [34] F. Sun, F. Zhang, F. Zhao, X. Zhou, S. Pu, Chem. Phys. Lett., 380, 206 (2003).
- [35] S. Kobatake, M. Morimoto, M. Irie, Mol. Cryst. Liq. Cryst., 431, 523 (2005).
- [36] S. Spagnoli, D. Block, E. Botzung-Appert, I. Colombier, P. L. Baldeck, A. Ibanez, A. Corval, J. Phys. Chem. B, 109, 8587 (2005).
- [37] A. Spangenberg, R. Metiver, J. Conzalez, K. Nakatani, P. Yu, M. Cirroud, A. Leaustic, R. Guglielmetti, T. Uwada, T. Asahi, Adv. Mater., 21, 309 (2009).
- [38] J. Piard, R. Metvier, M. Cirroud, A. Leaustic, P. Yu, K. Nakatani, New J. Chem., 33, 1420 (2009).
- [39] A. Patra, R. Metivier, F. Briset, K. Nakatani, Chem. Commun., 48, 2489 (2012).
- [40] J. Su, J. Chen, F. Zeng, Q. Chen, S. Wu, Z. Tong, Polym. Bulletin, 61, 425 (2008).
- [41] A. Patra, R. Metivier, J. Piard, K. Nakatani, Chem. Commun., 46, 6385 (2010).
- [42] S. Rath, M. Heilig, H. Port, J. Wrachrup, Nanolett., 7, 3845 (2007).
- [43] T. Mizokuro, H. Mochizuki, A. Kobayashi, S. Horiuchi, N. Yamamoto, N. Tanigaki, T. Hirada, Chem. Mater., 16, 3469 (2004).
- [44] T. Feczko, K. Samu, K. Wenzel, B. Neral, B. Voncina, Color Technol. 129, 18 (2012).
- [45] T. Feczko, O. Varga, M. Kovacs, T. Vidoczy, B. Voncina, J. Photochem. Photobiol. A, 222, 293 (2011).
- [46] T. Feczko, M. Kovacs, B. Voncina, J. Photochem. Photobiol. A, 247, 1 (2012).
- [47] D. Li, M. Zhang, G. Wang, S. Hing, New J.Chem., 38, 2348 (2014).
- [48] M. G. Zhu, L. Zhu, J. J. Han, W. Wu, J. K. Hurst, A. D. Q. Li, J. Am. Chem. Soc., 128, 4303 (2006).
- [49] L. Ma, Q. Wang, G. Lu, R. Chen, X. Sun, Langmuir, 26, 6702 (2010).
- [50] F. D. Benedetto, E. Mele, A. Canposo, A. Athanassiou, R. Cingolani, D. Pisignano, Adv. Mater., 20, 314 (2008).
- [51] A. Bianco, G. Iardino, A. Manuelli, C. Bertarelli, G. Zerbi, ChemPhysChem, 8, 510 92007).
- [52] K. Jeong, S. Park, Y. D. Lee, C. K. Lim, J. Kim, B. H. Chung, I. C. Kwon, C. R. Park, S. Kim, Adv. Mater., 25, 5574 (2013).
- [53] S. Rath, M. Heilig, E. Al-Khalisi, T. Klingler, H. Port, J. Lumin., 108, 401 (2004).
- [54] S. J. Lim, B. K. An, S. D. Jung, M. A. Chung, S. Y. Park, Angew. Chem. Int. Ed., 116, 6506 (2004).
- [55] L. Y. Zhu, W. W. Wu, M. Q. Zhu, J. J. Han, J. K. Hurst, A. D. Q. Li, J. Am. Chem. Soc., 129, 3524 (2007).
- [56] E. Jares-Erijman, L. Giordano, C. Spagnudo, K. Lidke, T. M. Jovin, Mol. Cryst. Lig. Cryst., 430, 257 (2004).
- [57] I. L. Medintz, S. A. Trammell, H. Mattoussi, J. M. Mauro, J. Am. Chem. Soc., 126, 30 (2004).

- [58] H. Furukawa, M. Misu, K. Ando, H. Kawaguchi, Macromol Rapid Commun., 29, 547 (2008).
- [59] J. Chen, F. Zeng, S. Wu, Q. Chen, Z. Tong, Chem. Eur. J., 14, 4851 (2008).
- [60] J. Chen, F. Zeng, S. Wu, J. Q. Zhao, Q. Chen, Z. Tong, Chem. Commun., 43, 5580 (2008).
- [61] J. Chen, F. Zeng, S. Wu, J. Su, Z. Tong, Small, 5, 970 (2009).
- [62] J. Chen, P. Zhang, X. Yu, X. Li, Y. Tao, P. Yi, J. Macromol. Sci. Part A, 48, 637 (2011).
- [63] Y. Lv, H. Liu, B. Zhao, Z. Tian, A. D. Q. Li, Isr. J. Chem., 53, 294 (2013).
- [64] M. Q. Zhu, G. F. Zhang, C. Li, M. P. Aldred, E. Chang, R. A. Drezek, A. D. Q. Li, J. Am. Chem. Soc., 133, 365 (2011).
- [65] E. J. Harbron, Isr. J. Chem., 53, 256 (2013).
- [66] S. Kim, S. J. Yoon, S. Y. Park, J. Am. Chem. Soc., 134, 12091 (2012).
- [67] Y. Osakada, L. Hanson, B. Cui, Chem. Commun., 48, 3285 (2012).
- [68] Z. Hu, Q. Zhang, M. Xue, Q. Sheng, Y. G. Liu, Opt. Mater., 30, 851 (2008).
- [69] J. Chen, P. Zhang, G. Fang, P. Yi, F. Zeng, S. Wu, J. Phys. Chem., 116, 4354 (2012).
- [70] G. Feng, D. Ding, K. Li, J. Liu, B. Liu, Nanoscale, 6, 4141 (2014).
- [71] Y. H. Sheng, A. D. Peng, H. B. Fu, X. Y. Liu, Y. S. Zhao, Y. Ma, J. N. Yao, Nanotechnology, 18, 145707 (2007).
- [72] X. Sheng, Y. Qian, J. Nanosci. Nanotechn., 10, 8307 (2010).
- [73] F. M. Raymo, Isr. J. Chem., 53,247 (2013).
- [74] Y. Jin, N. Friedman, J. Am. Chem. Soc., 127, 11902 (2005).
- [75] W. H. Binder, R. Sachsenhofer, C. J. Straif, R. Zirbs, J. Mater. Chem., 17, 2125 (2007).
- [76] M. Piech, M. C. George, N. S. Bell, P. V. Braun, Langmuir, 22, 1379 (2006).
- [77] M. Piech, N. S. Bell, Macromolecules, 39,915 (2006).
- [78] N. Katsonis, T. Kudernac, M. Walko, S. J. van der Molen, B. J. van Wees, B. L. Feringa, Adv. Mater., 18, 1397 (2006).
- [79] J. Folling, S. Polyakova, V. Belov, A van Blaaderen, M. L. Bossi, S. W. Hell, Small, 4, 134 (2005).
- [80] D. Genovese, M. Montalti, L. Prodi, E. Rampazzo, N. Zaccheroni, O. Tosic, K. Altenhoner, F. May, J. Mattay, Chem. Commun., 47, 10975 (2011).
- [81] F. May, M. Peter, A. Hutten, L. Prodi, J. Mattay, Chem. Eur. J., 18, 814 (2012).
- [82] J. Jeong, E. Yun, Y. Choi, H. Y. Jung, S. J. Chung, N. W. Song, B. H. Chung, Chem. Commun., 47, 10668 (2011).
- [83] H. Okada, N. Nakajiama, T. Tanaka, M. Iwamoto, Angew. Chtm., 117, 7399 (2005).
- [84] L. Muhlstein, J. Sauer, T. Bein, Adv. Funct. Mater., 19, 2027 (2009).
- [85] M. Tomasulo, I. Yildiz, F. M. Raymo, Australian J. Chem., 59, 175 (2006).
- [86] L. Zhu, M. Q. Zhu, J. K. Hurst, A. D. Q. Li, J. Am. Chem. Soc., 127, 8968 (2005).
- [87] M. Tomasulo, I. Yildiz, F. M. Raymo, Inorg. Chim. Acta, 360, 938 (2007).
- [88] E. M. Lee, S. Y. Gwon, Y. A. Son, S. H. Kim, Spectrochim. Acta A, 97, 699 (2012).
- [89] E. M. Lee, S. Y. Gwon, Y. A. Son, S. H. Kim, Spectrochim. Acta A, 97, 806 (2012).
- [90] V. A. Barachevsky, O. I. Kobeleva, A. O. Ayt, A. M. Gorelik, T. M. Valova, M. M. Krayushkin, V. N. Yarovenko, K. S. Levchenko, V.

- V. Kiyko, G. T. Vasilyuk, Optical materials, 35, 1805 (2013).
- [91] Z. Erno, I. Yildiz, B. Gorodetsky, F. M. Raymo, N. R. Branda, Photocem. Photobiol. Sci., 9, 249 (2010).
- [92] S. A. Diaz, L. G. O. Menedez, M. H. Etchehon, L. Giordano, T. M. Jovin, E. A. Jares-Erijman, ACS Nano, 5, 2795 (2011).
- [93] S. A. Diaz, L. Giordano, T. M. Jovin, E. A. Jares-Erijman, NANO let., 12, 3537 (2012).
- [94] S. A. Diaz, G. O. Menendez, M. H. Etchehon, L. Giordano, T. M. Jovin, E. A. Jares-Erijman, ACS Nano, 5, 2795 (2011).
- [95] S. A. Diaz, L. Giordano, J. C. Azcarate, T. M. Jovin, J. Am. Chem. Soc., 135, 3208 (2013).
- [96] L. Dworak, A. J. Reuss, M. Zastrow, K. Ruck-Braun, J. Wachtveitl, Nanoscale, 6, 14200 (2014).
- [97] N. Bouchonville, A. Le Cigne, A. Sukhanova, M. Molinari, I. Nabiev, Laser Phys. Lett., 10, 085901 (2013).
- [98] C. Zhang, H. P. Zhou, L. Y. Liao, W. Feng, W. Sun, Z. X. Li, C. H. Xu, C. J. Fang, L. D. Sun, Y. W. Zhang, C. H. Yan, Adv, Mater, 22, 633 (2010).
- [99] T. Wu, J. C. Boyer, M. Barker, D. Wilson, N. R. Branda, Chem. Mater., 25, 2495 (2013).
- [100] J. C. Boyer, C. J. Carling, S. Y. Chua, D. Wilson, B. Johnsen, D. Baillie, B. D. Gates, N. R. Branda, Chem.-Eur. J., 18, 3122 (2012).
- [101] T. Wu, M. Barker, K. M. Arafeh, J. C. Boyer, C. J. Carling, N. R. Branda, Angew. Chem. Int. Ed, 52, 1106 (2013).
- [102] B. F. Zhang, M. Frigoli, F. Angiuli, F. Vetrone, J. Capobianco, Chem. Commun., 48, 7244 (2012).
- [103] Z. Chen, L. Zhou, W. Bing, Z. Zhang, Z. Li, J. Ren, X. Qu, J. Am. Chem. Soc., 136, 7498 (2014).
- [104] C. Zhang, C. H. Xu, L. D. Sun, C. H. Yan, Chem. Asian J., 7, 2225 (2012).
- [105] C. J. Carling, J. C. Boyer, N. R. Branda, Org. Biomol. Chem., 10.6159 (2012).
- [106] C. J. Carling, J. C. Boyer, N. R. Branda, J. Am. Chem. Soc., 131, 10838 (2009).
- [107] J. C. Boyer, C. J. Carling, B. D. Gates, N. R. Branda, J. Am. Chem. Soc., 132, 15766 (2010).
- [108] T. Yang, Q. Liu, S. Pu, Z. Dong, C. Huang, F. Li, Nano Research, 5, 494 (2012).
- [109] Z. Zhou, H. Hu, H. Yang, T. Yi, K. Huang, M. Yu, F. Li, C. Huang, Chem. Commun., 4786 (2008).
- [110] H. Yamaguchi, K. Matsuda, M. Irie, J. Phys. Chem. C, 111, 3853 (2007).
- [111] H. Nishi, T. Asahi, S. Kobatake, ChemPhysChem, 13, 3616
- [112] O. I. Kobeleva, T. M. Valova, V. A. Barachevsky, M. M. Krayushkin, B. V. Lichitskii, A. A. Dudinov, O. Yu. Kuznetsova, G. E. Adamov, E. P. Grebennikov, Optics and Spectroscopy, 109. 101 (2010).
- [113] M. M. Krayushkin, B. V. Lichitskii, A. A. Dudinov, O. Yu. Kuznetsova, O. I. Kobeleva, T. M. Valova, V. A. Barachevsky, Rus. Chem. Bull., 59, 1047 (2010).
- [114] V. A. Barachevskii, O. I. Kobeleva, T. M. Valova, A. O. Ait, L. S. Kol'tsova, A. I. Shienok, N. L. Zaichenko, A. V. Laptev, A. A. Khodonov, O. Yu. Kuznetsova, A. A. Dudinov, B. V. Lichitskii, M. M. Krayushkin, Theoret. Exper. Chem., 48, 14 (2012).
- [115] A. L. Baudrion, A. Perron, A. Veltri, A. Bouhelier, P. M. Adam, R. Bachelot, Nano Lett., 13, 282 (2013).
- [116] M. L. Ho, Y. P. Yu, Y. T. Chen, M. H. Lin, CrystEngComm., 14, 4049 (2012).

- [117] A. Ghavidast, N. O. Mahmoodi, M. A. Zanjanchi, J. Mol. Liq., 198, 128 (2014).
- [118] A. Ghavidast, N. O. Mahmoodi, M. A. Zanjanchi, J. Mol. Struct., 1048, 166 (2013).
- [119] M. Dohi, T. Tsujioka, Appl. Phys. Express, 6, 091601 (2013).
- [120] B. I. Ipe, S. Mahima, K. G. Thomas, J. Am. Chem. Soc., 125, 7174 (2003).
- [121] J. Cao, S. Wu, B. Shai, Q. Wang, J. Li, X. Ma, Dyes and Pigments, 103, 89 (2014).
- [122] O. Ivashenko, J. T. van Herpt, B. L. Feringa, P. Rudolf, W. R. Browne, J. Phys. Chem., 117, 18567 (2013).
- [123] Y. Shirashi, K. Tanaka, E. Shiracawa, Y. Sugano, S. Ichikawa, S. Tanaka, T. Hirai, Angew. Chem. Int.Ed., 52, 8304 (2013).
- [124] Y. Shirashi, E. Shiracawa, K. Tanaka, H. Sakamoto, S. Ichikawa, T. Hirai, Appl. Mater. Interface, 6, 7554 (2014).
- [125] A. M. Kelley, Nano Lett., 7, 3235 (2007).
- [126] S. Simoncelli, M. J. Roberti, B. Araoz, M. L. Bossi, P. F. Aramendia, J. Am. Chem. Soc., 136, 6878 (2014).
- [127] D. Liu, W. Chen, K. Sun, K. Deng, W. Zhang, Z. Wang, X. Jiang, Angew. Chem. Int. Ed., 50, 4103 (2011).
- [128] K. Matsuda, M. Ikeda, M. Irie, Chem. Lett., 33,456 (2004).
- [129] H. Yamaguchi, K. Matsuda, M. Ikeda, M. Irie, Bull. Chem. Soc. Jpn, 79, 1413 (2006).
- [130] A. Perrier, F. Maurel, J. Aubard, J. Phys. Chem., 111, 9688 (2007).
- [131] T. Kudernac, S. J. van der Molen, B. J. van Wees, B. L. Feringa, Chem. Commun., 3597 (2006).
- [132] T. C. Pijper, T. Kudernac, W. R. Browne, B. L. Feringa, J. Phys. Chem., 117, 17623 (2013).
- [133] H. Nishi, S. Kobatake, Macromolecules, 41, 3995 (2008).
- [134] H. Nishi, T. Asahi, S. Kobatake, J. Phys. Chem. C, 113, 17359 (2009).
- [135] H. Nishi, T. Asahi, S. Kobatake, J. Phys. Chem. C, 115, 4564 (2011).
- [136] H. Nishi, T. Namari, S. Kobatake, J. Mater. Chem., 21, 17249 (2011).
- [137] H. Nishi, T. Asahi, S. Kobatake, Phys. Chem. Chem. Phys. 14, 48984564 (2012).
- [138] H. Nishi, S. Kobatake, Dyes and Pigments, 92, 847 (2012).
- [139] S. Imao, H. Nishi, S. Kobatake, J. Photochem. Photobiol. A, 252, 37 (2013).
- [140] Y. Tsuboi, R. Shimizu, T. Shoji, N. Kitamura, J. Am. Chem. Soc., 131, 12623 (2009).
- [141] B. Wu, K. Ueno, Y. Yokota, K. Sun. H. Zeng, H. Misawa, J. Phys. Chem. Lett., 3, 1443 (2012).
- [142] R. Yasukuni, R. Boubekri, J. Grand, N. Feligj, F. Maurel, A. Perrier, R. Metivier, K. Nakatani, P. Yu, J. Aubard, J. Phys. Chem. C, 116, 16063 (2012).
- [143] T. Ochial, K. Isozaki, F. Pincella, T. Taguchi, K. I. Nittoh, K. Miki, Appl. Phys. Express, 6, 102001 (2013).
- [144] A. Spangenberg, R. Metivier, R. Yasukini, K. Shibata, A. Brosseau, J. Grand, J. Aubard, P. Yu, T. Asahi, K. Nakatani, Phys. Chem. Chem. Phys., 15, 9670 (2013).
- [145] J. Zhang, J. K. Whitesell, M. A. Fox, Chem. Mater., 13, 2323 (2001).
- [146] A. Manna, P. L. Chen, H. Akiyama, T. X. Wei, K. Tamada, W. Knoll, Chem. Mater., 15, 20(2003).
- [147] S. I. Yang, K. H. Kim, D. Kang, S. W. Joo, Photochem. Photobiol. Sci., 8, 31 (2009).

**DE GRUYTER OPEN** 

- [148] O. Tsutsumi, K. Yamamoto, K. Ohta, K. Fujisawa, K. Uno, T. Hashishin, C. Yogi, K. Kojima, Mol. Cryst. Liq. Cryst., 550, 105 (2011).
- [149] S. M. Shah, C. Martini, J. Ackerman, F. Fages, J. Colloid Interface Sci., 367, 109 (2012).
- [150] A. Miniewicz, J. Girones, P. Karpimski, B. Mossety-Lezczak, H. Galina, M. Dutkiewicz, J. Mater. Chem. C, 2, 432 (2014).
- [151] D. Dulic, S. J. van der Molen, T. Kudernac, H. T. Jonkman, J. J. D. de Jong, T. N. Bowden, J. van Esch, B. L. Feringa, B. J. van Wees, Phys. Rev. Lett., 91, 207 (2003).
- [152] N. Katsonis, T. Kudernac, M. Walko, S. J. van der Molen, B. J. van Wees, B. L. Feringa, Adv. Mater., 18, 1397 (2006).
- [153] S. J. van der Molen, J. Liao, T. Kudernac, J. S. Agustsson, L. Bernard, M. Calame, B. J. van Wees, B. L. Feringa, C. Schonenberger, Nano Lett., 9, 76 (2009).
- [154] M. Ikeda, N. Tanifuji, H. Yamaguchi, M. Irea, K. Matsuda, Chem. Commun., 13, 1355 (2007).
- [155] B. L. Feringa, J. Org. Chem., 72, 6635 (2007).
- [156] G. Xu, Q. D. Yang, F. Y. Wang, W. F. Zhang, Y. B. Tang, N. B. Wong, S. T. Lee, W. J. Zhang, C. S. Lee, Adv. Mater., 23, 5059 (20011).
- [157] R. F. Khairutdinov, M. E. Itkis, R. C. Haddon, 4, 1529 (2004).
- [158] A. C. Whalley, M. L. Steigerwald, X. Guo, C. Nuckolis, J. Am. Chem. Soc., 129, 12590 (2007).
- [159] Y. He, Y. Yamamoto, W. Jin, T. Fukushima, A. Saeki, S. Seki, N. Ishil, T. Aida, Adv. Mater., 22, 829 (2010).
- [160] A. Staykov, D. Nozaki, K. Yoshizawa, J. Phys. Chem. C, 11, 3517 (2007).

- [161] P. Bluemmel, A. Setaro, C. Malty, S. Reich, J. Phys.: Condens. Mater., 24, 394005 (2012).
- [162] E. Malic, A. Setaro, P. Bluemmel, C. F. Sanz-Navarro, P. Ordejon, S. Reich, A. Knorr, J. Phys.: Condens. Mater., 24, 394006 (2012).
- [163] T. Sendai, S. Biswas, T. Aida, J. Am. Chem. Soc., 135,11509 (2013).
- [164] S. Remy, S. M. Shah, C. Martini, G. Poize, O. Margeat, A. Heynderickx, J. Ackerman, F. Fages, Dyes and Pigments, 89, 266 (2011).
- [165] J. Massaad, Y. Coppel, M. Sliva, M. L. Kahn, C. Coudrett, F. Gauffre, Phys. Chem. Chem. Phys., 16, 22775 (2014).
- [166] A. Parrot, G. Izzet, L. M. Chamoreau, A. Proust, O. Oms, A. Dolbecq, K. Hakouk, H. E. Bekkachi, P. Deniard, R.Dessapt, P. Mialane, Inorg. Chem., 52, 11156 (2013).
- [167] L. Dworak, M. Zastrow, G. Zeyat, K. Ruck-Braun, J. Wachtveitl, J. Phys.: Condens. Mater., 24, 394007 (2012).
- [168] K.Nakatani, P. Yu, Adv. Mater., 13, 1411 (2001).
- [169] H. Zhang, T. Yi, F. Li, E. Delahaye, P. Yu, R. Clement, J. Photochem. Photobiol. A, 186, 173 (2007).
- [170] Y. Zou, S. Xiao, T. Yi, H. Zhang, F. Li, C. Huang, J. Phys. Org. Chem., 20, 975 (2007).
- [171] K. M. Yeo, C. J. Gao, K. H. Ahn, I. S. Lee, Chem. Commun., 4622 (2008).
- [172] H. Simizu, M. Ocubo, A. Nakamoto, N. Kojima, Inorg. Chem., 45, 10240 (2006).